Joni Tuomi

Fuse protection optimization of drive DC link

Metropolia University of Applied Sciences

Master of Engineering

Electrical and Automation Engineering

Thesis

30.11.2018

Author Title	Joni Tuomi Fuse protection optimization of drive DC link
Number of Pages Date	63 pages + 10 appendices 30 November 2018
Degree	Master of Engineering, M. Eng.
Degree Programme	Electrical and Automation Engineering
Specialisation option	
Instructors	Mika Asikainen, Design Manager Jukka Karppinen, Senior Lecturer Jarno Varteva, Principal Lecturer

This thesis is done for ABB Drives and the study examines the effectiveness of the fuse protection with different fuse alternatives. During a short circuit, the temperatures and energies can rise extremely fast and an uncontrolled short circuit can cause significant damage to devices as well as cause a risk for the safety of personnel. With correct protection methods, the maximum current and duration of short circuit can be limited to milliseconds, which prevents the damage or at least minimizes the amount of damage to the protected drive system.

In this thesis protection of four parallel connected drive modules is examined using ANSYS Simplorer simulation program. The focus of the study is primarily on simulating the current distribution in different parts of the system and optimizing the protection of the drive DC link. The simulation results are compared to calculations to verify the reliability of the simulation model.

The study compares how adding fuses to the DC link affects the operating times of fuses and the total energy in the circuit. In addition, the impact of 6-pulse and 12-pulse connection to the current share during short circuit is compared in the results.

Based on simulations, the fuse protection operates sufficiently with two DC link fuses, when the goal is to minimize the risks to personnel and system components. The selected protection concept is however affected by the requirements of the drive system. The sufficient fuse protection must also be verified with other methods, such as calculations and testing.

Keywords	Variable speed drive, Fuse, Short circuit protection, Simulation, DC link

Metropolia
University of Applied Sciences

Tekijä	Joni Tuomi
Otsikko	Sulakesuojauksen optimointi taajuusmuuttajan DC-välipiirissä
Sivumäärä	63 sivua + 10 liitettä
Aika	30 Marraskuu 2018
Tutkinto	Insinööri (ylempi AMK)
Koulutusohjelma	Sähkö- ja automaatiotekniikka
Suuntautumisvaihtoehto	
Ohjaajat	Mika Asikainen, Suunnittelupäällikkö Jukka Karppinen, Lehtori Jarno Varteva, Yliopettaja

Tämä opinnäytetyö on tehty ABB:n Drives-yksikölle ja työssä tutkitaan sulakesuojauksen toimivuutta erilaisilla sulakevaihtoehdoilla. Oikosulun aikana lämpötilat ja energiamäärät voivat kasvaa erittäin nopeasti ja oikosulku voi hallitsemattomana aiheuttaa suuria laitevahinkoja sekä henkilövaaraa. Oikealla suojausperiaatteella oikosulun maksimivirta sekä oikosulun kesto saadaan pienennettyä millisekunteihin, jolloin varsinaista komponenttivahinkoa suojattavalle laitteelle ei ehdi syntyä, tai ainakin vahingot jäävät pieniksi.

Tässä työssä tutkitaan neljän rinnankytketyn taajuusmuuttajamoduulin suojausta käyttäen apuna ANSYS Simplorer simulointiohjelmaa. Tutkimuksen pääpaino on erityisesti taajuusmuuttajamoduuleja yhdistävän DC-välipiirin läpi kulkevien virtojen mallintamisessa sekä sen optimaalisessa suojauksessa. Työssä verrataan simuloinnin tuloksia laskemalla saatuihin arvoihin, joilla simulointimallin luotettavuutta saadaan varmennettua.

Tutkimuksessa verrataan kuinka sulakkeiden lisääminen DC-välipiiriin vaikuttaa sulakkeiden toiminta-aikoihin ja samalla piirissä kulkevaan kokonaisenergiaan. Lisäksi tarkastellaan mikä vaikutus 6-pulssi- ja 12-pulssikytkennällä on piirin virranjakaumaan oikosulkutilanteessa.

Simulointitulosten perusteella sulakesuojaus saadaan toimimaan riittävän nopeasti kahdella välipiirin DC-sulakkeella, kun tavoitteena on henkilö- ja komponenttivahinkojen minimointi. Valittavaan ratkaisuun vaikuttavat kuitenkin taajuusmuuttajajärjestelmän vaatimukset. Lisäksi suojauksen toimivuus on aina varmistettava myös muilla menetelmillä, kuten laskennalla sekä testeillä.

| Avainsanat | Taajuusmuuttaja, Sulake, Oikosulkusuojaus, Simulointi, DC-välipiiri |

Metropolia
University of Applied Sciences

Acknowledgements

Metropolia
University of Applied Sciences

Contents

Metropolia
University of Applied Sciences

Appendices

Symbols, Subscripts and Abbreviations

Symbols

A	Conductor cross section
B	Magnetic flux density
H	Magnetic field intensity
c	Voltage correction factor
C	Capacitance
D	Diode
f	Frequency
I	Current
L	Inductance
R	Resistance
t	Time
U	Voltage
X	Reactance
Z	Impedance
κ	Factor for the calculation of the peak short-circuit current
ω	Supply angular frequency $= 2 \cdot \pi \cdot f$
θ	Electrical angle at which the short circuit current begins
ϕ	Power factor angle of the circuit impedance
μ	Permeability of the medium
τ	Time constant $=$ L/R

Subscripts

c	clearing
ic	Fuse let through (current)
C	Capacitor
D	DC
MAX	Maximum
rms	Root mean square
S	*Supply*
F	fuse
n	Nominal
k	Short circuit
p	Peak

T	Transformer
Q	Network
p	prospective RMS (short circuit current)
s	Maximum value of short circuit current
dc	Value of DC component

Superscripts

"	Subtransient
'	Transient

Abbreviations

ABB	Asea Brown Boveri
AC	Alternating Current
ANSYS	Analysis System
CSA	Canadian Standards Association
DC	Direct Current
Du/dt	The derivative of voltage with respect to time
EMC	Electromagnetic Compatibility
ESL	Equivalent Series Inductance
ESR	Equivalent Series Resistance
GTO	Gate Turn-Off Thyristor
HV	High Voltage
i^2t	Fuse melting integral
IEC	International Electrotechnical Commission
IGBT	Insulated-Gate Bipolar Transistor
LV	Low Voltage
MOS	Metal-Oxide-Semiconductor
RMS	Root Mean Square
R_{SC}	Short Circuit Ratio
SCR	Silicon Controlled Rectifier
UL	Underwriters Laboratories
X/R-ratio	Ratio of the system reactance to the system resistance.

1   Introduction

1.1   Background

This thesis is written for ABB`s System Drives product group. The basis for the study is with the help of simulation models and theoretical background to investigate which fuse protection methods are optimal for the DC short circuit protection of parallel connected variable speed drives. At the beginning of the study different DC protection concepts were estimated and few options were then chosen for a closer look. The amount and location of fuses are different in each option, which can have a considerable effect on the short circuits and fuse operation times in the event of a short circuit. On the other hand, some of the additional fuses can have only a little or no effect on the fuse operating times of the whole system.

To find out the behavior of the currents and voltages in the system, the key parameters for each part of the system were calculated and estimated for the simulation model. Since some of the components in the system doesn`t contribute significantly to the short circuit, it was also estimated which are the key components when determining the equivalent circuit for short circuit calculations. It is not reasonable to accurately simulate all components in a circuit because this would cause simulations to slow down. Therefore one challenge is to determine the sufficient accuracy level for reliable results.

The simulation models were created with ANSYS Simplorer simulation software. The simulation is considered necessary in addition to the calculations, because of the complexity of the system. The contribution of parallel connected modules increases the number of parameters and the changes in variables such as voltage, frequency, and impedance during short circuit makes it difficult to have reliable results only with theoretical calculations.

1.2   Scope of the Study

Calculations are mainly based on IEC standards such as IEC 60909, which defines the methods of calculating short-circuit currents in three-phase AC systems. This thesis focuses on specific drive modules, so many of the component values and parameters can be found from the data sheets as well as from the existing measurements of the components, which can then be used to find out the behavior of the system during a short circuit.

On the other hand, this means that the proposed solutions may not be valid when other components or other types of drive modules are used. The purpose of this thesis is not to optimize the cost of the components or to find new components. The priority is to find to the most optimal short circuit protection concept by varying the placements, amounts, and ratings of the existing components.

1.3　Goals

The objective of the thesis is to create a reliable equivalent circuit for short circuit simulations and then using the simulation model to find the most optimal DC fuse protection solutions. These simulations and calculations are used as a generic solution for both 6-pulse and 12-pulse configurations of parallel connected drive modules. The goal is also to make the simulation models of components and systems as accurate as possible so that the simulation model of the system could be then used also later on in different kinds of simulation cases.

The protection of the system must be sufficient for the most demanding short circuit circumstances. The simulation parameters are chosen so that the contribution of the external parameters such as the supply grid, transformers and motor loads are taken into account. Also, both the highest expected short circuit currents as well as the lowest short circuit currents are evaluated and used as a basis for the comparison of protection concepts.

2 AC Drive

Motors need electrical energy to generate torque and speed. These parameters can be adjusted by variable speed drive or AC drive, which is the most common control method for the motor, mainly because of low investment and maintenance costs of AC drives as well as the good operating performance. The AC drive adjusts the required electrical energy to match the energy needed by the motor using rectifiers, DC capacitors, and inverters. (ABB Drives, 2011)

AC Drive converts the alternating current to direct current for the DC link with rectifier consisting of IGBT:s, thyristors or diodes. Direct current made by the rectifier is however pulsating and is filtered by the DC capacitors in the DC link, which reduces ripple and smoothens the current. The DC link supplies the inverters that convert the DC back to AC current, which then has proper frequency and voltage amplitude for the application requirements. Inverters typically consist of IGBT:s that produce the desired waveform. The converted electrical power is then used to run the AC motor. The motor speed can be adjusted by increasing or decreasing the output frequency of the AC drive. AC drives provide many benefits, such as energy and cost savings as well as increased performance and reliability of the system. (What is an AC drive)

3   Drive System Components

In addition to the drive itself, the drive system consists of all components from the sup-
plying network to the load. Drive system as a whole can be complex. Similarly short
circuit currents of AC drive are influenced by the components of the drive, but also other
variables in the system such as supply grid, motor and the load, which means that esti-
mating system short circuit currents can also be complicated. This chapter focuses only
those parts of the drive system, which are the most relevant to the short circuit calcula-
tions. Therefore drive system components such as EMC- and du/dt-filters, which smooth-
ens the voltage and current, but don`t have a significant contribution to short circuit cur-
rents, are not included in this chapter.

3.1   Supply Grid

Supply grid includes generators, transmission lines, and distribution network. Properties
of these grid components define the quality of the electrical supply for the drive system,
including the behavior in short circuits. One way to define the properties of the supply
grid is the strength of the power system, which describes the stability of the system in
different operating conditions and is defined as the ability of the system to maintain its
voltage during various types of disturbances. Stronger systems experience less voltage
changes, while weak systems experience more undesirable effects such as voltage var-
iations. Strong power systems also typically have higher fault currents compared to
weaker systems. High currents following a fault can be viewed as a grid responding
strongly to a voltage drop to keep the voltage stable. The voltage distortion also depends
on the strength of the power system. The higher the ratio, the lower the voltage distortion
and low system strength typically leads to increased volatility of network voltages in both
normal and disturbance conditions. (AEMO)

System strength is measured by the available fault current, which is the maximum short
circuit current in an unprotected circuit or by the short circuit ratio R_{SC}. Short circuit ratio
determines how quickly dc component of a fault current decays in short circuit. Higher
the ratio, the more slowly dc component decays. Strong networks have relatively low
impedances compared to weak networks and have high short circuit ratios. System im-
pedances are caused by generators, transformers, transmission lines and loads. Precise
R_{SC} level is often not known, so the estimated R_{SC} values are typically used, which can
be different from the actual values (Wang & Lemmon, pp. 2-4)

Standard IEC-60909-0, Short-circuit currents in three-phase a.c. systems, describes the equivalent circuit for supply grid used in short circuit calculations. The equivalent circuit is shown in Figure 1. (Schlabbach, 2005, p. 46)
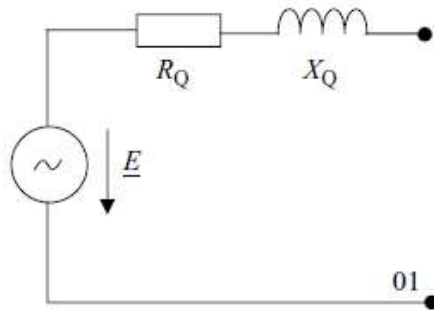

Figure 1. Equivalent circuit of supply grid *(Schlabbach, 2005, p. 46)*

Network impedance Z_Q can be calculated in case of a three-phase symmetrical short circuit with the equation (1) if the initial short circuit current I_K'' and nominal voltage U_n are known. (International Electrotechnical Commission, 2016, p. 23)

$$Z_Q = \frac{c \cdot U_n}{\sqrt{3} \cdot I_k''} \qquad (1)$$

If precise values for network parameters are not available, values $R_Q = 0,1 \cdot X_Q$ and $X_Q = 0,995 \cdot Z_Q$ can be used for the calculation of network resistance and reactance when short circuit impedance of the network Z_Q is known. The resistance has to be considered especially when the peak-short circuit current I_p or the DC-component I_{DC} need to be calculated. (International Electrotechnical Commission, 2016, p. 24)

3.2   Transformer

A transformer is a device consisting of two or more windings that are connected to each other by a strong magnetic field. The design requirements depend on the application. For power transformers, the main requirement is to transfer the electric power at a constant frequency and minimal power losses, while the voltage is being changed from one level to another. (ABB, 2010, p. 11)

The operation of a transformer is based on electromagnetic induction. A sinusoidal voltage applied to the primary windings creates a magnetizing current, which induces a voltage to the secondary windings of the transformer in a relation between the number of turns in the primary and secondary side of the transformer in no load conditions. (ABB, 2010, p. 12)

Transformers can be divided into power transformers and distribution transformers. Power transformers support the transmission of energy over long distances at high voltages and the distribution transformers are needed when energy is distributed from substations to various users. Variable speed drive transformer is a type of distribution transformer that is used for the voltage transformation as well as the electric isolation necessary for low voltage drives. Variable speed transformers are normally fed by medium voltage network from 5 kV to 36kV and they convert the supply voltage for converters from 400 V to 4 kV supply voltages. Transformers are typically oil insulated or dry-type depending on the application. (ABB, 2010, pp. 32-41)

There are three basic ways to connect the phase windings of the three-phase transformer. In Y- connection or wye, the one end of three-phase winding is connected to the neutral point. The Y-connection is the natural choice for the highest voltages and when the neutral is intended for loading. In D-connection or delta, the three-phase windings are connected in series and form a ring. D-connection is advantageous in large power transformers, where there the current is high and the voltage relatively low. The third basic way for transformer connection is the Z-connection, or zigzag, which can be used as a secondary winding when the current in a D-connected winding is small and the required dimension of the winding conductor is inconveniently small to handle in a factory. Different types of three-phase windings are shown in Figure *2*. (ABB, 2010, pp. 162-163)
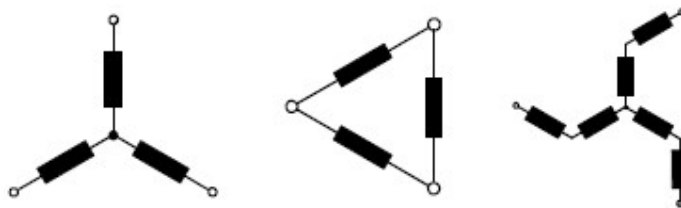

Figure 2. Windings of three-phase transformer *(ABB, 2010, p. 162)*

Arranging the connection of transformer windings in different ways, it is possible to make a voltage displacement between the sides of the transformer. A 12-pulse system is made by two 6-pulse systems, where one of the secondary windings is in star and the other one in delta connection with 30 degrees phase shift between primary and secondary. 12-pulse connection cancels 5th and 7th harmonic currents and so the voltage ripple of 12-connection is significantly smaller than in 6-pulse connection. (ABB, 2010, pp. 57-62)

Transformer`s impedance and configuration have an effect on the short circuit currents in the system. Out of the network parameters, the transformer usually has the biggest impact on the short circuit currents. Transformer`s no-load impedance Z_0 is not constant but will vary non-linearly with the applied voltage due to the linearity of the magnetizing curve. The impedance of the circuit Z is the short-circuit voltage divided by the rated current. These impedances Z_0 and Z are connected parallel in an equivalent diagram. Since no-load impedance Z_0 is typically significantly larger than Z, the total impedance in parallel connection can be considered as Z. The real part of Z_0 represents no-load losses, while the real part of Z represents the load losses of the transformer. (ABB, 2010, p. 13)

The equivalent circuit of supply transformer used in short circuit calculations is a series connection of the total resistance and reactance of the transformer as shown in Figure 3.
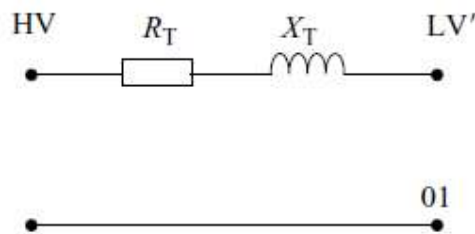

Figure 3. Transformer equivalent circuit according to IEC-60909-0 *(Schlabbach, 2005, p. 47)*

When the nominal apparent power of the transformer S_n and short circuit impedance z_k are known, short circuit resistance r_k and reactance x_k can be calculated with equations (2) and (3) follows. (International Electrotechnical Commission, 2016, p. 25)

$$r_k = \frac{P_k}{S_n}$$

(2)

$$x_k = \sqrt{z_k^2 - r_k^2} \tag{3}$$

Transformer`s resistance and reactance can be then calculated using short circuit resistance and reactance by using equations (4) and (5). (International Electrotechnical Commission, 2016, p. 25)

$$R_T = r_k \cdot \frac{U^2}{S_N} \tag{4}$$

$$X_T = x_k \cdot \frac{U^2}{S_N} \tag{5}$$

3.3 Fuse

Fuses protect the system against the effects of overcurrent by melting fuse elements and thus opening the circuit. Diodes, thyristors and other semiconductor components in AC drive require very fast-acting fuses, so-called semiconductor fuses. The fuse element of the semiconductor fuse is usually made from a highly conductive material, such as silver or copper with regions of reduced cross-sectional areas that melt quickly during a short circuit. The type of these weak spots defines the fuses characteristics and how the fuse behaves in different load situations. (Eaton, 2016, pp. 2-4)

The element is surrounded with sand or quartz type filling material, which quenches the arc when reduced element sections melt. Surrounding material conducts heat away from the material and forms a glassy material with very high resistance, which then isolates the current flow and ends the short circuit. The fuse element and the arc quenching element are enclosed inside a ceramic fuse body, which is made of ceramic or engineering plastic. The ceramic body withstands the high temperature and pressure formed during a short circuit and has good mechanical strength. The fuse body also has good dielectric strength as it can withstand the increased voltages without losing its insulating properties. (Eaton, 2016, p. 4)

To connect the fuse to the protected circuit, the fuse also has end fitting or connectors, end plates, and other necessary parts depending on the type and construct of the fuse,

as well as the manufacturing methods used. Typical semiconductor fuse construction is shown in Figure 4. (Eaton, 2016, p. 4)
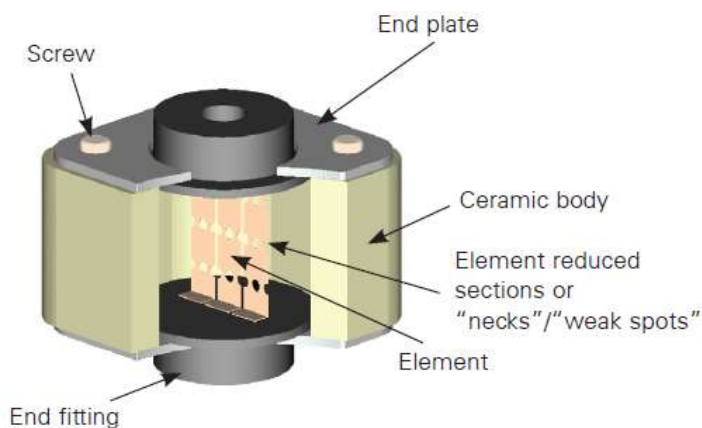

Figure 4. Semiconductor fuse construction (Eaton, 2016, p. 4)

For currents up to the maximum rating, the fuse dissipates the generated heat and the fuse element temperature stays low. During overload, the temperature of the fuse element rises. If the overload is allowed to continue, it will eventually cause fuse element to start to melt. The time it takes for fuse element to melt depends on the amount of overcurrent and is shorter with higher overcurrents. Because of the long heating times, the overload current can usually be characterized by the RMS-value. Most semiconductor fuses are however not designed to protect the circuit against long-duration overloads. (Eaton, 2016, p. 5)

Short circuits can cause the available RMS value of available short circuit current to go to more than 20 times the normal operating current of the system. Under these heavy overloading or short circuit circumstances, the temperature of the fuse element reaches the melting point almost instantaneously and melts well before the current would reach its unrestricted fault current. Without the protective device, the damage to the system can occur in milliseconds, which is of the same order as the duration of an AC half cycle. (Eaton, 2016, p. 5)

The time it takes from the initiation of the fault to the element melting is called pre-arcing time. During the pre-arcing phase, the resistance and fuse voltage are low and the short circuit current rises very rapidly and reaches its peak let through current value at the end of pre-arcing. Figure 5 shows how total clearing time of the fuse can be divided into a

pre-arcing time where current quickly rises to its maximum value and an arcing time, where current rapidly quenches. (Eaton, 2016, p. 5)
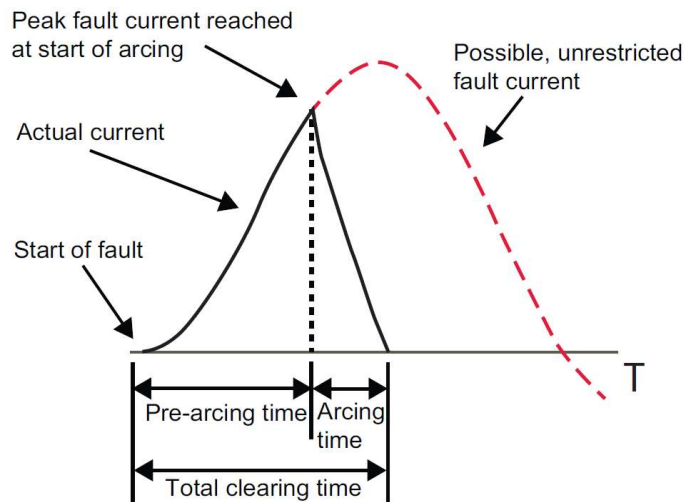

Figure 5. Pre-arcing and arcing currents of fuse in short circuit. (Eaton, 2016, p. 5)

Arcing phase begins when the melting of the element causes an arc being formed at element restrictions. High resistance arc interrupts the heavy currents and the voltage across the fuse increases rapidly. The arc also tends to burn the fuse element away from the restrictions, which further increases the resistance and arc length and these cumulative effects isolate the circuit quickly and extinct the arc. Figure 6 shows the fuse current and voltage in typical short circuit conditions. (Eaton, 2016, p. 5)
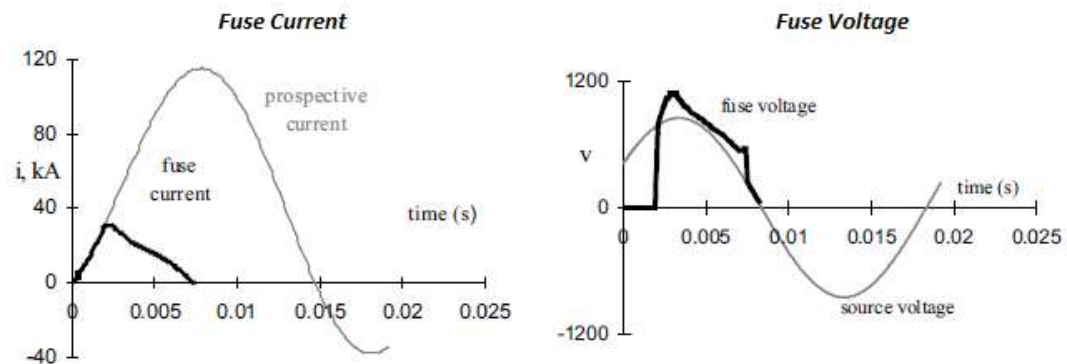
Figure 6. Example of fuse currents and voltages in short circuit. (Mersen, 2011, p. 13)

When the objective of the fuse protection is to minimize the let-through energy, the fuse should generate high arc voltage. However, in power electronic circuit the diodes, thyristors and other semiconductors can experience this arc voltage in a non-conducting state,

which determines that the peak arc voltage must be lower than inverse voltage withstand capacity of the semiconductor device. (Mersen, 2011, p. 13)

Peak let through current is not always sufficient for determining the fuse protection for the system, since two fuses can have the same let through current rating, but different total clearing times. Fuse clearing i²t takes into account both let through current and clearing time and it is the integral of the square of the current multiplied by the time the current flows. Clearing i²t is proportional to the total amount of energy released during the fault. Relative i²t energy during the clearing time t_c can be represented by the following equation (6). (Mersen, p. 34)

$$I_{RMS}^{2}(t_c) = \int_0^{t_c} I_{RMS}^{2}\, dt \tag{6}$$

Usually, the RMS is dropped from the equation and is simplified as shown in equation (7):

$$i^2 t = \int_0^t i^{\,2} dt \tag{7}$$

Because of the nearly triangular shape of the fuse current curve, the total clearing i²t can also be estimated with sufficient accuracy by calculating the area of the triangle shown in Figure 7. (Mersen, 2011, p. 13)

$$\text{Total let through } i^2 t = \frac{\text{Peak current}^2 \cdot \text{Total clearing time}}{3} \tag{8}$$
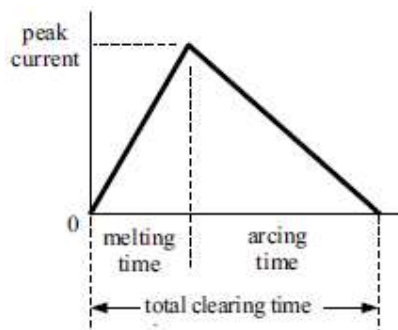

Figure 7. Approximated fuse current in short circuit (Mersen, 2011, p. 13)

In modern applications, many systems involve both AC and DC and the majority of the applications involving DC, have an AC supply, which is rectified to supply a load. The

applications that utilize DC to AC inverters, such as AC drives, can be considered in two parts for fusing. First the AC to DC converter and then the inverter section. (Eaton, 2016, p. 18)

Usually, fuse ratings are defined for the AC currents. If AC fuses are used in DC protection, the fuse selection becomes more complex. The fuse values in DC application may be either higher or lower than in AC application because in DC circuits the fuse operation is based on different conditions than in AC circuits. In a DC circuit, the inductance limits the rate of current rise. The time spent for the current to reach 63 percent of the final value is called time constant τ and it is referred to in terms of L/R. (Eaton, 2016, p. 21)

In many rectifier circuits, a fuse will even under fault conditions be subjected to an AC voltage. In these conditions, the extinguishing of the arc is assisted by the voltage reducing to zero. In DC application the voltage, under which the fuse can safely operate depends on circuit time constant. When time constant is short, the DC voltage rating can be greater than the AC voltage rating. However, for most fuses, the DC voltage rating is significantly less than the AC voltage rating and this DC rating further decreases as the circuit time constant increases. (Eaton, 2016, p. 21)

When fuses are dimensioned for inverter protection, the fuses should have the fastest possible operating times, which will meet the current requirement and are also rated with DC voltage capability at least as high as the DC link voltage. Because of the magnitude of the fault current from the capacitor and small inductance in the circuit, the current rise time may be very high, which makes I^2t selection criteria more difficult as device or fuse data may not be available for operating times below 3 milliseconds. For this reason, the selection typically is based on the lowest I^2t that will meet the requirements. Even when the device protection is not ensured, this fuse selection will certainly limit the damage to all the circuit components. (Eaton, 2016, p. 28)

Low I^2t value of the fuse is also important when the capacitor has a low value. When a short circuit occurs in the inverter, the capacitors discharge and the current rises rapidly to a peak value and will then decay. It is important that the fuse has opened and cleared before the voltage on the capacitor decays to a low value. Otherwise, the fuse may not have developed sufficient insulation resistance to withstand the DC link voltage when it is replenished from the supply. (Eaton, 2016, p. 28)

Figure 8 shows the equivalent circuit of the fuse with series connected fuse resistance R, fuse inductance L and fuse voltage V_F
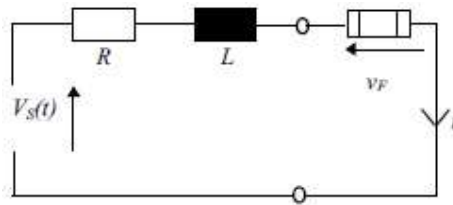

Figure 8. Fuse equivalent circuit (Mersen, 2011, p. 13)

3.4   Rectifier Unit

The most common rectifier circuit in three-phase AC Drive is the 6-pulse diode rectifier, which consists of six diodes and a choke. Together with a DC capacitor, the diode-diode bridge forms a low-pass filter for smoothing the DC-current. The choke can be either on the DC- or AC-side. The 6-pulse rectifier is simple and cost-effective, but it generates a high amount of low order harmonics 5th, 7th and 11th especially with a small smoothing inductance. Unlike for other semiconductors, it is not possible to control the current strength. (ABB Drives, 2017, p. 16)

Disturbances caused by the harmonic content can be reduced by increasing the pulse number. The 12-pulse rectifier is formed by connecting two 6-pulse rectifiers in parallel that feeds the DC link. The waveform of 12-pulse connection is smoother because of lower amounts of low order harmonics than in 6-pulse connection. In 12-pulse connection, the transformer secondaries have a 30° electrical degree phase shift between each other, which eliminates 5th and 7th harmonics and thus reduces the voltage ripple. Figure 9 shows DC voltages for 6-pulse and 12-pulse connections. (ABB Drives, 2009)
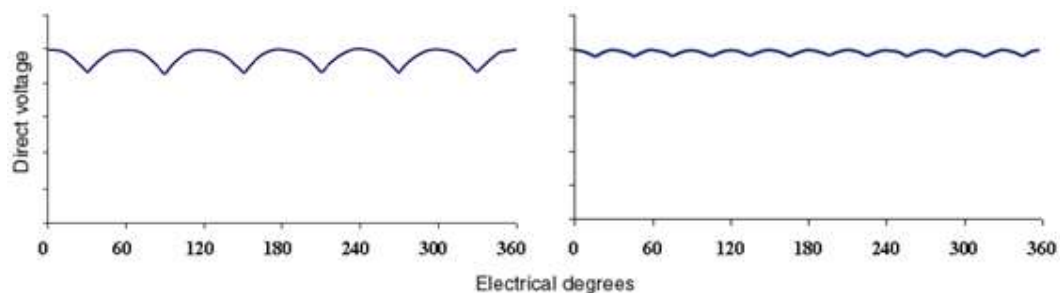

Figure 9. Direct voltage in 6-pulse and 12-pulse connection. *(ABB, 2010, pp. 58-59)*

Semi-controlled rectifiers consist of three thyristors and three diodes. Compared to the diode-diode bridge, the diode-thyristor bridge provides the possibility to control the current flowing in the forward direction by either allowing or blocking the current. By controlling the firing angle of the thyristors, the DC voltage can be increased gradually, allowing the smooth charging of the DC link capacitors without an additional charging circuit. Like diode-diode rectifier, diode-thyristor rectifier is able to deliver power from the AC network to the DC link, but not in the opposite direction. (ABB Drives, 2015, p. 19)

A fully controlled rectifier is accomplished by replacing the diodes in a 6-pulse rectifier with thyristors. A thyristor is controlled by a triggering pulse for the transition from a nonconducting to a conducting state, so the phase angle at which the thyristor starts to conduct can be delayed. Delaying the firing angle over 90°, the DC link voltage turns negative, which allows a regenerative power from the DC link back to the power supply. It is more common to connect another thyristor bridge antiparallel with the first one, which allows the current polarity reversal. In this configuration, the first bridge conducts in rectifying mode and the other in regenerating mode. (ABB Drives, 2017, p. 17)

IGBT supply unit allows both rectification and regeneration, and it makes it possible to control the DC-voltage level and displacement power factor separately regardless of the power flow direction. The result is nearly sinusoidal supply current with low harmonic content. IGBT supply unit causes high-frequency common mode distortion of the phase to neutral and phase to ground voltages. Dedicated filtering to suppress high-frequency content is needed to prevent interference. Typically LCL type of filters are used to filter the disturbances caused by the high switching frequencies. (ABB Drives, 2017, pp. 18-19)

Figure 10 shows an example of diode-thyristor rectifier circuit with three thyristor and three diodes for converting the AC voltage to DC as well as AC chokes for smoothening the current.
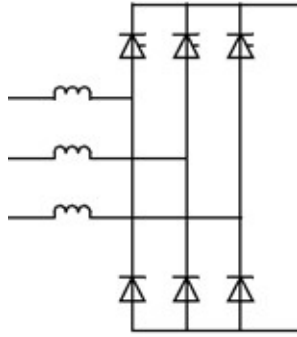
Figure 10. Diode-Thyristor rectifier circuit with AC chokes (ABB Drives, 2015, p. 20)

The ideal relation between the DC voltage in rectifier output and the supplied phase-to-phase AC voltage can be calculated from the one period of DC voltage pulse shown in Figure 11. The output DC voltage U_D is calculated with equation (9) as follows. (Electronic Power Conversion, Line-Frequency Diode Rectifiers)

$$U_D = U_{MAX} \cdot \frac{1}{\frac{\pi}{3}} \int_{\frac{\pi}{3}}^{\frac{2\pi}{3}} sinx \; dt \tag{9}$$

Solving the equation (9) gives the value of $1{,}35 \cdot U_{RMS}$ for the output voltage, which for example with a three-phase supply voltage of 690 V gives a DC voltage of 931,5 V that can be used in DC link calculations.

$$U_D = \frac{3}{\pi} \cdot U_{MAX} = \frac{3 \cdot \sqrt{2}}{\pi} U_{RMS} \approx 1{,}35 \cdot U_{RMS}$$
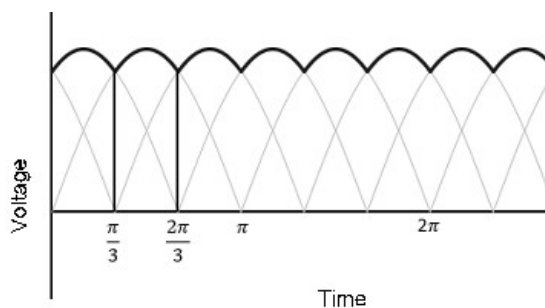
Figure 11. Ideal DC output voltage of 6-pulse rectifier with period duration of $\frac{1}{3}\pi$

There are several types of high power semiconductor devices available for AC drives. Diodes are able to conduct current in one direction and cannot be controlled. Thyristors can conduct current only in one direction, but the conducting is triggered on by a signal. For transistors, the on and off states can be controlled by a voltage signal. Figure 12 shows the semiconductor types and their typical applications. (ABB SACE, 2017, pp. 8-9)
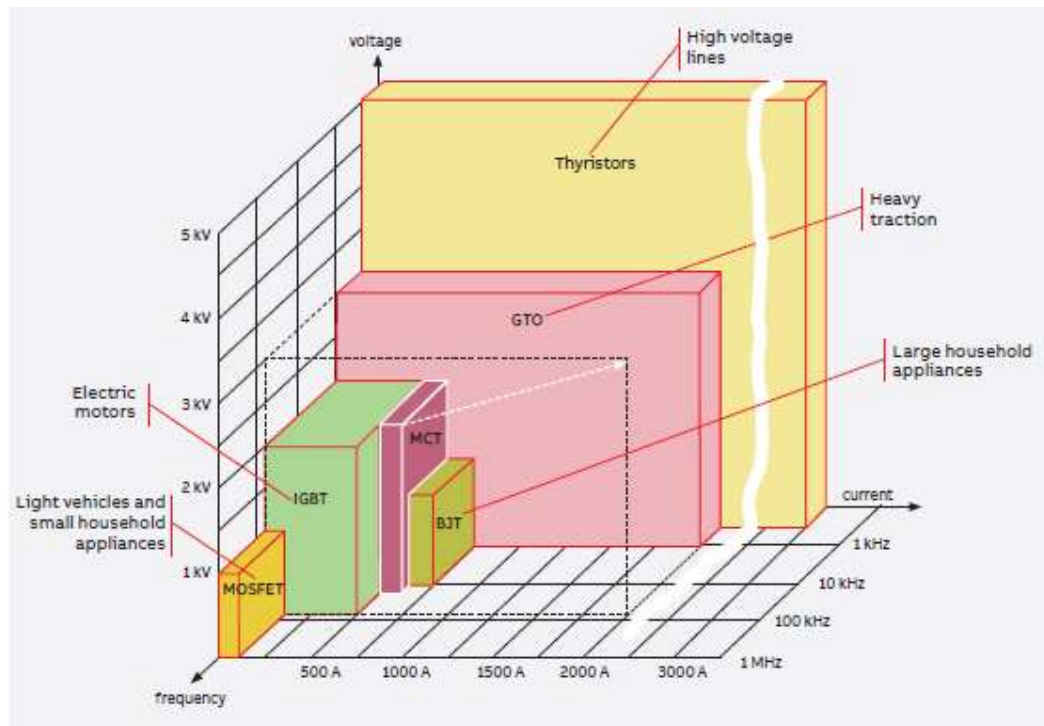

Figure 12. Applications of electronic components (ABB SACE, 2017, p. 9)

Thyristors (SCR) are silicon-controlled rectifiers that are not fully controllable, which means that the thyristors can be turned on, but cannot be turned OFF. Thyristors are switched on by a gate signal and it remains on even after the gate signal has been removed. Thyristor remains in the on state until it`s turned off by applying a reverse voltage to the terminals or when the forward current falls below a certain threshold value known as holding current. A thyristor behaves like a normal semiconductor diode after it has been turned on. (ABB SACE, 2015, p. 58)

A GTO (Gate Turn-Off thyristor) is a type of thyristor, which is a fully controllable switch that can be turned on and off by its gate. GTO can be turned on by a gate signal, but unlike thyristor, it can also be turned off. The main difference compared to normal thyristor is a special gate arrangement, which enables the interruption of the load current at

any point by applying negative current to the gate. However, the turning on of GTO is not as reliable as for thyristor and small positive gate current must be maintained even after turn on to improve reliability. (ABB SACE, 2015, pp. 58-59)

GTO thyristors have long switch-off times, which restrict the maximum switching frequency to approximately 1 kHz. This limitation of low switching frequency leads in case of inverters to a high content of harmonics in the AC signal. Figure 13 shows the symbol and equivalent circuit of GTO thyristor. (ABB SACE, 2015, pp. 58-59)
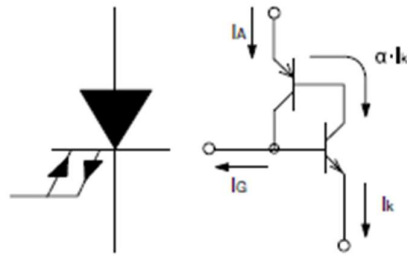
Figure 13. Symbol and equivalent circuit of GTO thyristor. (ABB SACE, 2015, p. 58)

The IGBT (Insulated Gate Bipolar Transistor) is a fairly recent invention. The first-generation IGBTs were in use during the 1980s and early 1990s. The current generation of IGBTs have high efficiency and fast switching properties. Current IGBTs are also small, inexpensive and the withstand short circuits for a certain limited period of time. In addition to variable frequency drives, these devices are also used for electric cars, trains, and air conditioners. (ABB SACE, 2015, pp. 59-60)

IGBT is a three-terminal power semiconductor with four alternating layers (P-N-P-N) that are controlled by a metal-oxide-semiconductor (MOS) gate structure without regenerative action. IGBTs cannot conduct in the reverse direction. In bridge circuits where a reverse current flow is needed, an additional freewheeling diode is required in parallel with the IGBT to conduct current in the opposite direction. Symbol and the equivalent circuit of IGBT is shown in Figure 14. (ABB SACE, 2015, pp. 59-60)
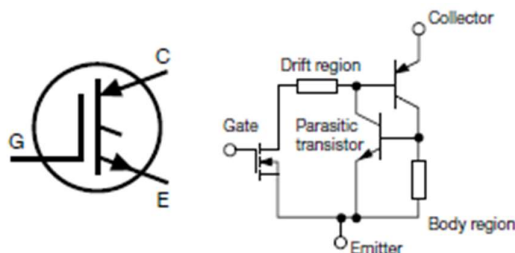

Figure 14. Symbol and equivalent circuit of an IGBT. (ABB SACE, 2015, pp. 59-60)

The equivalent circuit of the three-phase full-wave bridge rectifier consisting of diodes and thyristors can be modeled with ideal diodes as shown in Figure 15.
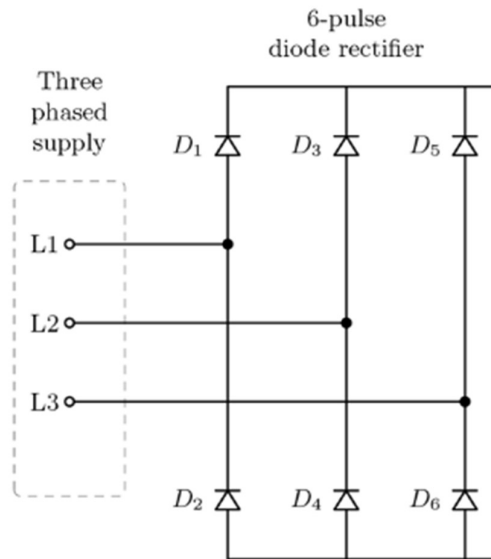

Figure 15. Equivalent circuit of rectifier. (Solbakken, 2017)

3.5   AC Choke

The harmonic distortion can be reduced by connecting AC choke in AC input or DC choke in DC bus of an AC drive. Chokes are usually ferrite core inductors, which can have high inductance values in small space. The AC choke smoothens the current waveform in the power supply and voltage in the DC link of the drive. The choke resists a change of current by storing energy in the magnetic field. It causes only very little resistance to continuous DC currents, but the magnetic field caused by the flowing current evens any rapid changes in current. (ABB Drives, 2017, p. 13)

Harmonic currents are created by non-linear loads that are connected to the power distribution system. Power electronic converters such as AC drive can increase harmonic disturbances by injecting harmonic currents directly into the grid. The voltage distortion with certain current distortion depends on the short circuit ratio R_{SC} of the supply. Higher short circuit ratio means lower voltage disturbances. When harmonic currents increase above certain limits, the effects can vary from overheating of transformers, cables, and motors to a failure of components. (ABB Drives, 2017, p. 4)

Increasing the inductance improves the situation. For example, optimum dimensioning of the DC choke can be reached when the product of the motor power in kW and the inductance in mH is close to 25. The effect of a choke in line current is shown in Figure 16. (ABB Drives, 2017, p. 13)
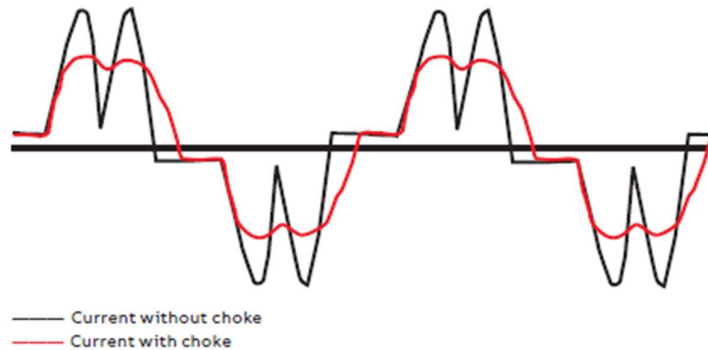

—— Current without choke
—— Current with choke

Figure 16. The effect of a choke on the line current. (ABB Drives, 2017, p. 13)

The inductance of a coil can be calculated by equation (10) when the permeability of the coil µ, number of turns N, cross-section A and length of the coil ℓ are known. (UNLV College of Engineering)

$$L = \frac{\mu \cdot N^2 \cdot A}{\ell} \qquad (10)$$

The magnetic field around the coil can be described by the magnetic flux density B and magnetic field intensity H. The flux density and the field intensity are in proportion to the permeability of the medium µ as shown in equation (11). (UNLV College of Engineering)

$$B = \mu \cdot H \qquad (11)$$

The magnetic field intensity H increases when the number of turns N around the coil or current is increased and respectively decreases as the length of the coil ℓ is increased as shown in equation (12). The parameters affecting the magnetic flux intensity are shown in Figure 17. (UNLV College of Engineering)

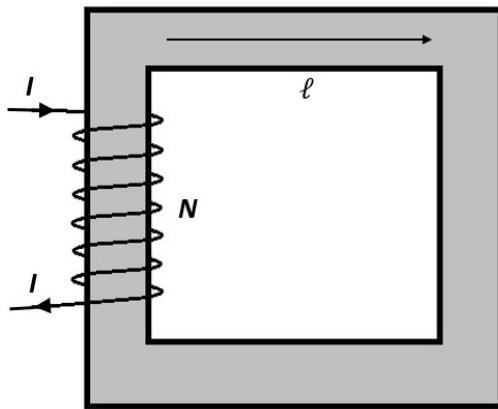$$H = \frac{N \cdot I}{\ell} \qquad (12)$$

Figure 17. Magnetic flux intensity H in a coil

Choke Saturation

Ferromagnetic materials have high permeability, which means that a relatively small number of magnetizing turns of the coil is required to obtain a strong magnetic field. Also, it means that considerably greater flux density is achieved in a ferromagnetic core than in an air coil with the same current. Unlike permeability of many other materials, the permeability of ferromagnetic materials is not constant. (ABB, 2010, p. 16)

When sinusoidal AC voltage is applied to the primary winding, a magnetizing current flows through the windings and magnetic flux floats in the core. The magnetic flux is also sinusoidal in shape, but is 90 degrees behind the applied voltage. The magnetizing current is not sinusoidal but considerably distorted. (ABB, 2010, p. 16)

The behaviour of a ferromagnetic core can be represented with B-H magnetization curve shown in Figure 18, which shows corresponding values of magnetic flux and magnetizing current during one cycle of the applied voltage. In starting point (a) the flux density and the magnetizing current have their maximum negative value. The magnetizing current and the magnetic flux then proceed toward smaller negative values and at point (b) the magnetizing current is zero, but there is still remanent magnetic flux in the core. The magnetizing force then starts to increase towards positive values and at point (c) the flux density in the core becomes zero. This value of the magnetizing force is called the coercive force. (ABB, 2010, p. 17)
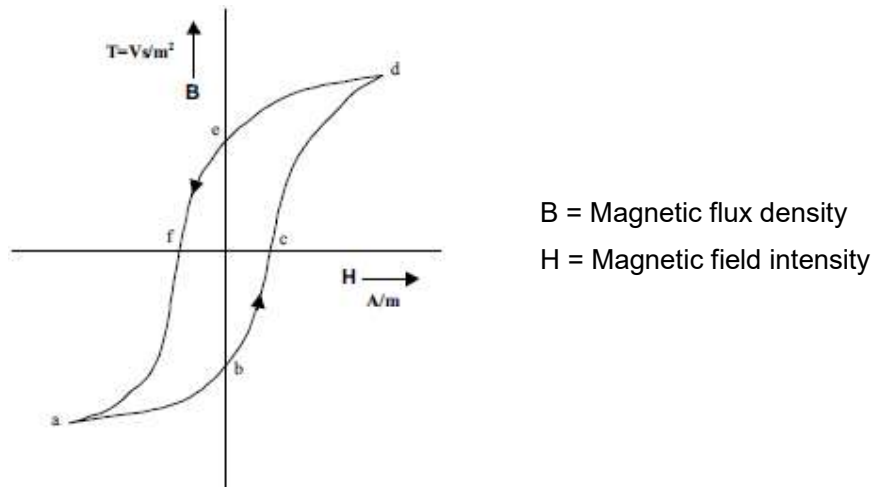
Figure 18. B-H magnetisation curve (ABB, 2010, p. 17)

When magnetizing force is further increased, a flux in the positive direction starts to float in the core and at point (d) the current and the flux start decreasing. However, the decreasing values follow the curve to the left towards (e) instead of the curve back towards (c). At point (e) the current is zero and there is now remanent flux floating in the opposite direction compared to the remanent flux in point (b). Increasing the current in the negative direction the flux decreases further and becomes zero at point (f). The flux then continues to increase in the negative direction until it reaches point (a), where the one cycle of applied voltage is completed. (ABB, 2010, p. 17)

The behaviour of magnetizing current is caused by numerous small magnets attached to the crystalline molecular structure of the ferromagnetic material. In the original state, these magnetic domains are randomly orientated and the magnetic field from each of them cancels each other out. If the material is placed in an external magnetic field, the domains start to change their direction toward the direction of the external field. Due to the magnetic domains that become unidirectional, the total magnetic field will be thousands of times higher than the original external field. (ABB, 2010, p. 17)

When the external field disappears, there will still remain a considerable amount of magnetic domains, which remain in the same direction. Reorientation of the domain is a gradual process that requires time, which is the reason why the magnetic flux lags behind the magnetic force. The hysteresis loop shows that the slope of the curve decreases with increasing magnetising force. At a certain flux density, the slope of the curve will become equal to the permeability of air, which means that no further increase in the magnetic field can be obtained from the ferromagnetic material. (ABB, 2010, pp. 17-18)

3.6   Inverter Unit

DC voltage created by the rectifier is converted to AC with a desired frequency by the inverter. First, the DC capacitors in the inverters smoothen the DC voltage by storing the energy when the voltage increases and discharging energy when the voltage decreases. The resulting waveform is shown in Figure 19.
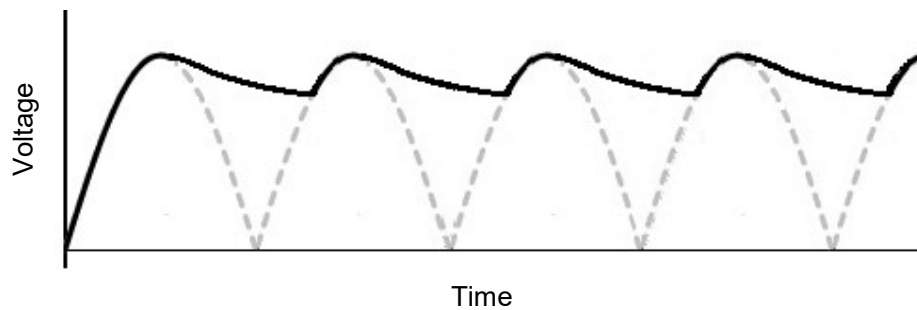

Figure 19. Effect of DC link capacitors on output voltage

The most often used inverter topology is the two-level inverter, which can have three output voltage levels -U, 0 and +U that are used to create the AC voltage. The benefits of two-level inverter include its high performance with relatively simple design and low cost. Inverters typically use six IGBT transistors that function as switches between positive and negative busbar. By controlling the switching of IGBTs, the inverter produces sinusoidal AC voltage with high frequency switching pulses that runs the AC motors with the torque or speed demanded by the application. Figure 20 shows an example of an inverter using pulse width modulation, where IGBTs control the length and frequency of the DC pulses.
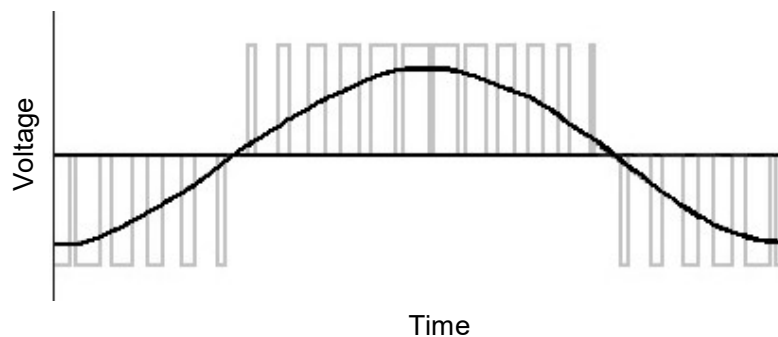
Figure 20. Voltage pulses resulting a sinusoidal voltage waveform in pulse width modulation

The inverter also protects the motor and itself from various faults, such as overloads. In applications, where high motor power is needed, the inverters can be connected in parallel. (Hietalahti, 2013, pp. 75-79)

Figure 21 shows the equivalent circuit of the capacitor in series with capacitor resistance and conductor impedance.

Figure 21. Equivalent circuit of capacitor with series DC resistance and conductor impedance (Schlabbach, 2005, p. 59)

3.7 Conductors

The conductors also have an effect on the currents and voltages of a drive system. Conductors, such as supply and motor cables, as well as drive busbars, adds resistance and inductance to the system. The type and size of the conductors are based on the current demand. Current-carrying capacity of a conductor depends on various factors, such as the type of cable, maximum allowed temperature of cable, ambient temperature, and the installation method. IEC standard 60364-5-52 shows current-carrying capacities for different cable types, as well as correction factors for different installation methods and conditions. Conductor impedance in an equivalent circuit can be expressed as a series connection of cable resistance, cable inductance and conductor joint.

The resistance of conductor R can be calculated with equation (13), when electrical resistivity ρ, length of the conductor ℓ, and conductor cross section A are known.

$$R = \rho \cdot \frac{\ell}{A} \tag{13}$$

Length of a conductor is dependent on the installation, while conductor cross-section is obtained based on the current-carrying capacity of the cable. The electrical resistivity of the conductor depends on the conductive material and the conductor temperature. Table 1 shows typical conductivity and resistivity values for aluminium and copper in 20 °C temperature.

Table 1. Material resistivity according to IEC60909-0 (International Electrotechnical Commission, 2016, p. 29)

Material	Resistivity [Ωmm²/m]
Copper	$\frac{1}{54} \approx 0{,}018$
Aluminium	$\frac{1}{34} \approx 0{,}029$
Aluminium alloy	$\frac{1}{31} \approx 0{,}032$

Cable conductors can be in different formations. In trefoil formation, conductors are in triangular shape and the distance between each conductor is the same. In flat formation, the distance between conductors next to each other is the same. These connector formations are shown in Figure 22. When the cable type is known, the inductance of cable L can be calculated with equation (14), when the correction factor of cable formation K, the distance between conductors s and radius of conductor r_c are known. (ABB, 2010, p. 23)

$$L = 0{,}05 + 0{,}2 \cdot \ln\left(\frac{K \cdot s}{r_c}\right) \qquad (14)$$
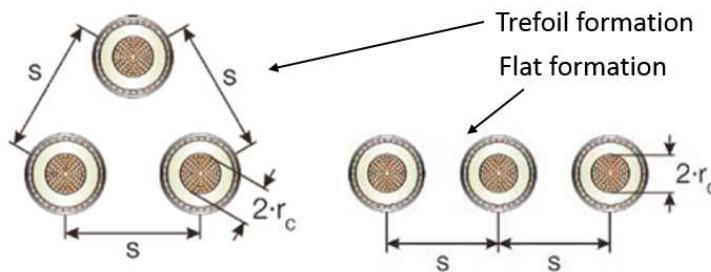
Figure 22. Trefoil and flat formation *(ABB, 2010, p. 23)*

Standard IEC 61363-1 defines cables in short circuit as a series connected resistance and inductance as shown in Figure 23. The cabling does not contribute to short circuit and only attenuates the short circuit currents, so the maximum values for short circuit are obtained when the cabling is as short as possible. Resistance and reactance values at conductor temperature 20 °C and rated frequency are sufficiently accurate for most of the cases. The resistance of conductor joint can be ignored with high short circuit currents.

$$R_c \qquad X_c$$

Figure 23. Simplified cable impedance in short circuit equivalent circuit

3.8 Motor Load

An electric motor converts electrical energy into mechanical energy. The main compo-
nents of the motor are stator and rotor. The rotor is the rotating part of the motor, which
is mounted on the motor shaft. The rotor is made of thin laminations, which hold the rotor
windings. The stator is the stationary part of the motor, which holds packages of lamina-
tions where the electrical windings are placed. The main components of a typical induc-
tion motor are shown in Figure 24. (Danfoss, 2014)
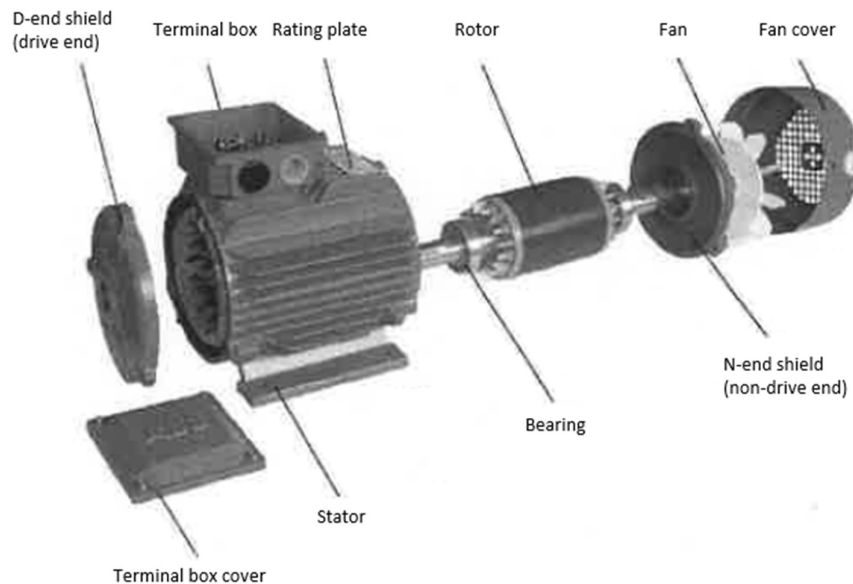
Figure 24. Motor breakdown of components *(Hietalahti, 2013, p. 138)*

During a short circuit motor contributes a small but noticeable addition to the short circuit
current regardless of the type and size of the motor. Voltage supply to the motor is no
longer stable and starts to decay. The magnetic field in the motor attempts to support
the reduced voltage by becoming a power source, which provides additional current to
the system. (Broussard, 2013)

The amount of additional current during a short circuit depends on the motor impedance. At the start of a short circuit, there is an asymmetrical current that contains both AC and DC components. Without a stable voltage supply, both AC and DC component decay and the motor and load inertia determine the rate of decay. (Broussard, 2013)

The motor impedance determines the AC component value. The resistive component in the motor impedance is much lower than the reactive component, so for the motor contribution, the reactive component provides a sufficient value. (Broussard, 2013)

The DC component`s rate of decay is determined by the X/R ratio of the system. When reactance X is closer to zero, the DC component is not noticeable and the current is symmetrical. If resistance R is small, the DC component decays slowly. Normally there are both resistance and reactive components in the system. (Broussard, 2013)

If the motor data is not available, the low voltage motor contribution can be assumed to be four times the rated full load current. The assumption is based on the contribution of 3,6 times rated current from induction motors and 4,8 times rated current from synchronous motors as well as the 75 % current contribution from induction motors and 25 % contribution from synchronous motors. (Broussard, 2013)

The equivalent circuit of a motor with total motor resistance R_M and total Reactance X_M is shown in Figure 25.
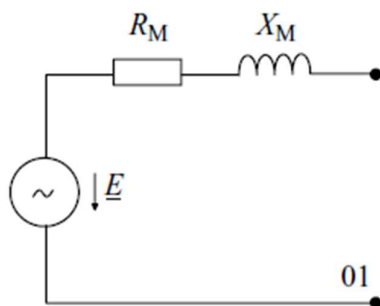

Figure 25. Equivalent circuit of asynchronous motor *(Schlabbach, 2005, p. 55)*

4   Short Circuit

When considering the properties of a system or component dimensioning, the behavior of the short circuit must be known in different parts of the network. Typically AC short circuit can be divided into three periods. During sub-transient period within the first cycles after the short circuit, the AC current is very high and falls rapidly. In a transient period, the current slows at a much slower rate before it reaches the steady-state period, where the current is no longer decreasing. The rate of which the DC component decays is dependent on the short circuit ratio R/X. AC short circuit currents in a function of time are shown in Figure 26.
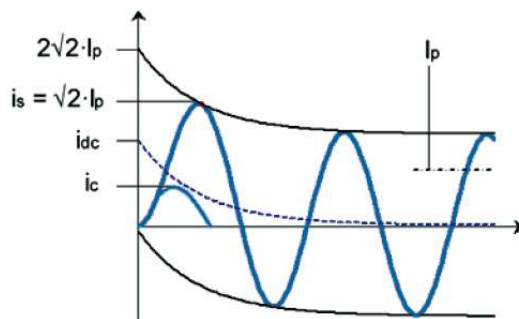
Figure 26. AC short circuit current with steady state AC component and decaying DC component *(ABB Low Voltage Switches, 2004, p. 28)*

In AC circuit, the short circuit current as a function of time at the short circuit location is given by equation (15), where the first term in the equation is the steady state AC short circuit current and the second term is a decaying transient DC component.

$$i(t) = \sqrt{2} \cdot I_p \cdot \left[sin(\omega t + \theta - \phi) - sin(\theta - \phi) \cdot e^{\frac{-\omega t}{tan\phi}} \right] \tag{15}$$

Peak short-circuit current I_p can be calculated with the equation (16) when factor κ and the initial three-phase short-circuit current I_K'' are known.

$$I_P = \kappa \cdot \sqrt{2} \cdot I_k'' \tag{16}$$

The factor κ can be calculated according to standard IEC60909-1 with the equation (17) as a function of R/X:

$$\kappa = 1{,}02 + 0{,}98 \cdot e^{-\frac{3R}{X}} \tag{17}$$

Combining equations (16) and (17) gives then maximum peak current in function of R/X shown in equation (18).

$$I_p = \sqrt{2} \cdot I_k'' \cdot \left(1{,}02 + 0{,}98 e^{-\frac{3R}{X}}\right) \tag{18}$$

The maximum value of the first asymmetrical peak current is obtained if the short circuit starts at purely inductive voltage angle θ = 0, when it can reach $2\sqrt{2}$ = 2,83 times the RMS symmetrical current or about 2,5 times the symmetrical RMS current in a circuit with an X/R ratio of 10:1. (Mersen, 2011, p. 11)

When calculating short circuit currents for specific applications, both maximum and minimum short circuit currents should be considered. Maximum short circuit current determines the capacity or rating of electrical components, while the minimum short circuit current is needed for example for the selection of fuses and setting the protective devices. (International Electrotechnical Commission, 2016)

Following conditions must also be taken into account based on IEC 60909-0, when calculating the maximum short circuit currents

- Voltage factor C_{max} is applied
- System configuration is chosen so that it leads to the maximum values of short circuit currents
- Impedances have been selected so that they correspond to the maximum short circuit contribution of the circuit.
- Motors are included in the simulation.
- Resistances of cables are modeled at a temperature of 20 °C.

The short circuit can be either 3-phase, line-to-line or line-to-earth. The highest currents are caused by three-phase short circuits, but line-to-line short circuits are usually more common. 3-phase and line-to-line short circuits are shown in Figure 27.
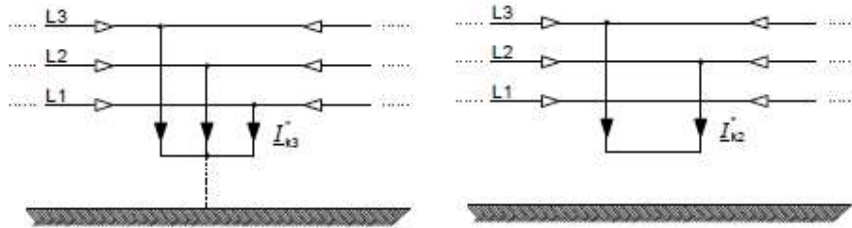
Figure 27. Three-phase short circuit and line-to-line short circuit *(International Electrotechnical Commission, 2016, p. 19)*

If the voltage factor c, nominal RMS line-to-line voltage U_n and three-phase short circuit impedance are known, the sub-transient three-phase short circuit current I_k'' can be calculated as follows in equation (19).

$$I_k'' = \frac{c \cdot U_n}{\sqrt{3} \cdot Z_k} = \frac{c \cdot U_n}{\sqrt{3} \cdot \sqrt{R_k^2 \cdot X_k^2}} \tag{19}$$

In the case of a line-to-line short circuit, the initial short circuit can be calculated by equation (20).

$$I_{k2}'' = \frac{\sqrt{3}}{|Z_1 \cdot Z_2|} \cdot \frac{c \cdot U_n}{\sqrt{3}} \tag{20}$$

If impedances Z_1 and Z_2 are equal, the relation between line-to-line and three-phase short circuit current can be shown in a relation of three-phase short circuit current as in equation (21)

$$I_{k2}'' = \frac{\sqrt{3}}{2} \cdot I_k'' \tag{21}$$

Direct current causes different problems than alternating current, especially since the arc extinction is more difficult. For alternating current, there is a natural passage of current through zero at each half cycle. With direct current there is no such natural passage, so to guarantee arc extinction, the current must be completely quenched. (ABB SACE, 2011, s. 12)

When the fault occurs in DC circuit, the current in the circuit increases exponentially as shown in Figure 28 and the growth rate depends on the circuit time constant L/R, where L is the inductance and R the resistance of the circuit. During one time constant τ the current reaches 63 % value of its maximum value. (Mersen, 2011, p. 12)
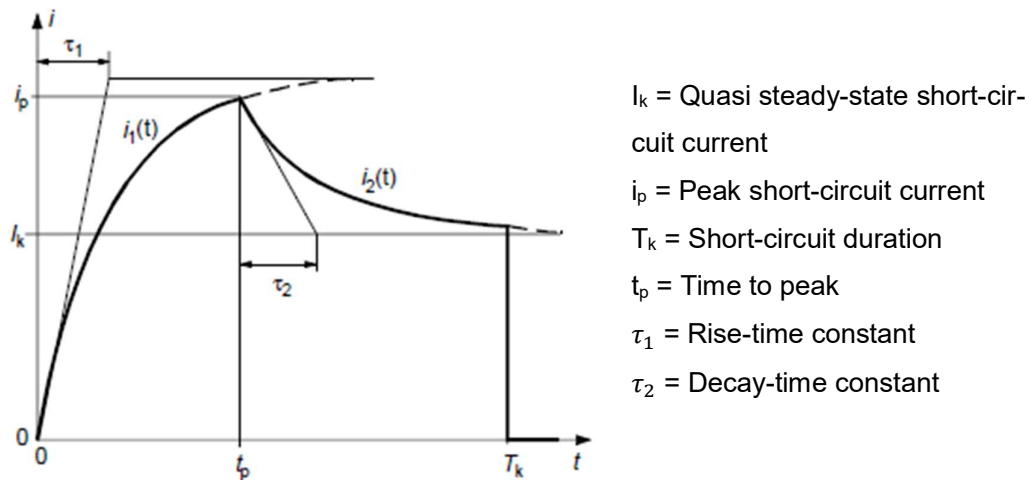

I_k = Quasi steady-state short-circuit current

i_p = Peak short-circuit current

T_k = Short-circuit duration

t_p = Time to peak

τ_1 = Rise-time constant

τ_2 = Decay-time constant

Figure 28. Short circuit currents in DC circuit. *(International Electrotechnical commission, 1997, s. 19)*

Instantaneous short circuit current in a DC circuit is given as a function of time by the equation (22). At the beginning of the short circuit, the current rises quickly and towards the end, the rate at which the current increases slows down towards the steady state current. The available constant short circuit current in a steady state is V_{dc}/R, where V_{dc} is the source voltage. (Mersen, 2011, p. 12)

$$i(t) = I \cdot (1 - e^{\frac{-Rt}{L}}) \tag{22}$$

When a short circuit occurs immediately downstream of the rectifier, which is usually the worst case considered for DC short circuit calculations, the fault resistance starts to decrease and the fault current is only limited by the impedances of upstream network and components. Even with fault resistances of 1 mΩ, the fault current can reach considerably high values, both in terms of DC capacitors´ discharge peak and also in terms of steady state value. These currents can be on a scale of 10 times the nominal current of the rectifier. Resulting values of the fault current would likely cause the breaking of the electrical components without protective devices. If two or more parallel transformers are

installed or cable size increased, the upstream AC impedance decreases further, resulting even higher short circuit currents. Short circuit current components during a short circuit on a DC side are shown in Figure 29. (ABB SACE, 2015, pp. 15-23)
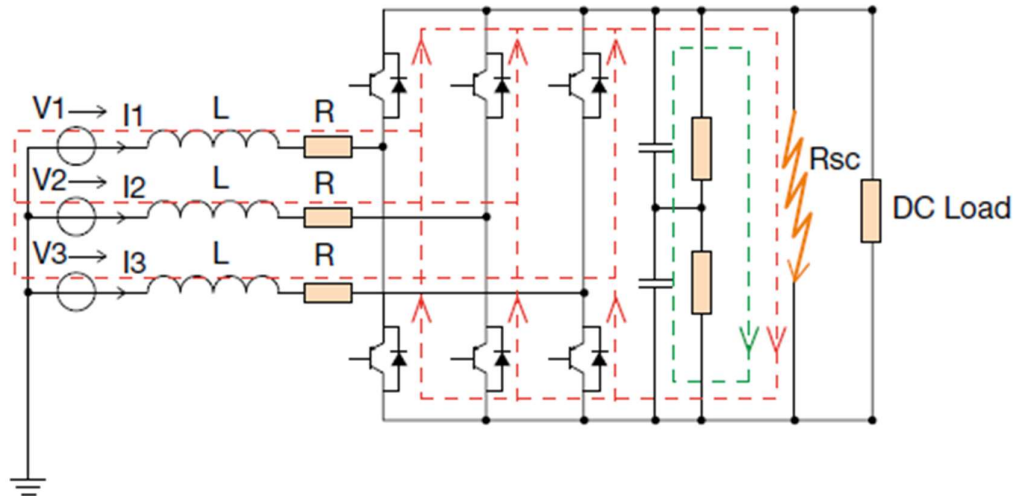

Figure 29. DC short circuit current components. (ABB SACE, 2015, p. 20)

5   Simulation Parameters

The drive that is studied consists of four drive modules, which each have diode-thyristor rectifiers, DC link capacitors, and IGBT inverters. In addition, the drive system components include supply transformers, AC and DC fuses and motor as shown in Figure 30. The contribution of these components on short circuit simulations are described later in this chapter.
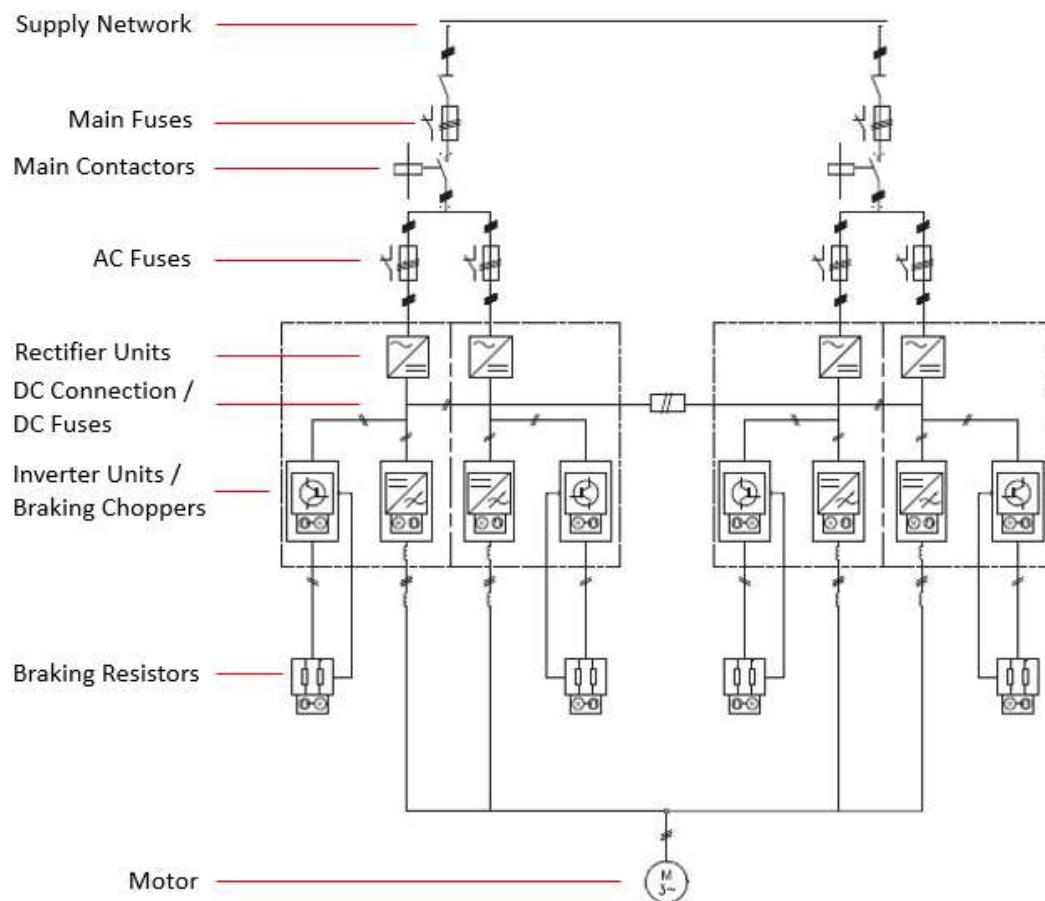
Figure 30. Drive main circuit (ABB Drives, 2017, p. 15)

Simulation parameters are chosen so that there would be the worst conditions for fuses. This means that the simulation parameters will give the highest possible short circuit currents, which are then the basis of the fuse selection. In short circuit calculations, also the lowest values are typically considered, but in most cases, the protection for low short circuit currents is much easier to arrange.

In the simulation model, disconnectors, breakers, contactors, and other switching devices are ideal switches, so in other words, they don`t have any parameters in the simulation that would have an effect on the short circuit behavior of the circuit in question.

Each drive has filters, such as EMC filters and common mode filters. The purpose of these filters is to maintain the sinusoidal current form as well as possible and thus prevent the disturbances in the system. Filters, however, are considered to have a low impact on short circuit currents and are neglected. Also grounding impedances does not have any significant effect on currents.

The AC drive can also have braking choppers and resistors. If a motor is rotating faster than is required by the frequency of the AC drive, the motor starts supplying energy back to the DC link. If braking functionality is active, the excess current is directed to braking resistors. Braking components, however, have only restricting effect on current and so the resistor braking would rather decrease the short circuit currents. The goal of the study is to find the highest values of short circuit currents, so the braking circuit is not included in the simulation model.

In normal operation, the current is divided in a drive module as shown in Figure 31. When the current in a DC side of the rectifier is set to 100 %, the AC line current is 82% and the current flowing through diodes are 82% compared to the DC current.
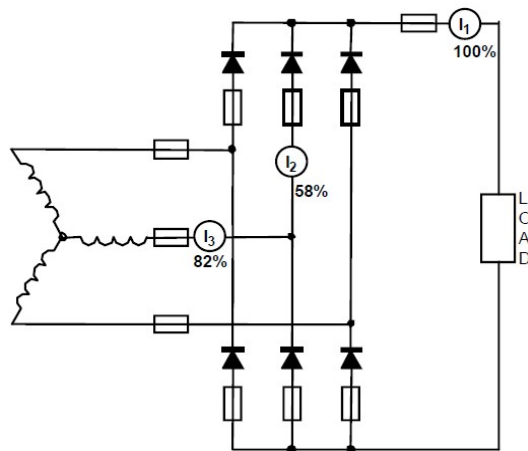
Figure 31. Current share in three-phase rectifier circuit (Eaton, 2016, p. 15)

5.1 Supply Grid

Network impedances are represented by adding impedance to an ideal network, which is transferred to the low voltage side of the transformer, shown in Figure 32. Network resistance and inductance are chosen so that the network has a 65 kA maximum allowable prospective RMS short circuit current I_K'' at the start of the short circuit and the maximum short circuit current during the first peak I_P is 143 kA.
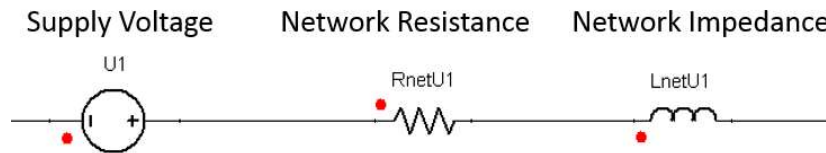

Figure 32. Supply network in short circuit simulation

Network tolerances have been taken into account by adding a correction factor of 1,10 to the supply voltage. This means that all modules and network components basically have an identical cabling, motor load, and other component parameters and the correction factor is added to compensate for any tolerances caused by imbalances. The correction factor is necessary for example for compensating the voltage variations and the lack of line capacitances and shunt admittances of non-rotating loads. Voltage correction factors that are based on short circuit condition requirements defined in standard IEC 60909-0 are shown in Table 2.

Table 2. Voltage factor c according to IEC 60909-0

Nominal system voltage U_n	Voltage factor c for the calculation of	
	maximum short circuit currents C_{max}	minimum short circuit currents C_{min}
Low voltage	1,05 (systems with ±6 % tolerance)	1,05 (systems with ±6 % tolerance)
100 V to 1 000 V	1,10 (systems with ±10 % tolerance)	1,10 (systems with ±10 % tolerance)

By using the supply voltage, the voltage correction factor and maximum short circuit current values, the network impedance can be calculated by using equation (1) as follows.

$$Z_Q = \frac{1,1 \cdot 400\ V}{\sqrt{3} \cdot 65\ kA} = 3,91\ m\Omega$$

R/X value can then be calculated by inserting maximum values for short circuit currents I_P = 143 kA, I_K'' = 65 kA and network impedance $Z_Q = 3{,}91 \; m\Omega$ to the equation (18), which then results in R/X value of 0,2 used in the simulation:

$$\frac{R}{X} = -\frac{ln\left(\frac{\frac{I_p}{I_K'' \cdot \sqrt{2}}-1{,}02}{0{,}98}\right)}{3} \approx 0{,}2$$

When network impedance and R/X values are known, the network reactance value can be calculated using equation (23) as follows.

$$Z_Q^2 = R_Q^2 + X_Q^2 \tag{23}$$

$$\Rightarrow X_Q = \frac{Z_Q}{\sqrt{1 + \left(\frac{R_Q}{X_Q}\right)^2}} = \frac{3{,}908 \; m\Omega}{\sqrt{1 + (0{,}2)^2}} \approx 3{,}83 \; m\Omega$$

Network resistance is then calculated using the equation (23), which gives the following value for the network resistance.

$$R_Q = \sqrt{Z_Q^2 - X_Q^2} \approx 0{,}77 \; m\Omega$$

Supply grid values used in simulation are shown in Table 3.

Table 3. Main parameters for supply grid.

Supply Voltage	U_n [V]	400
Voltage factor	c	1,1
Frequency	f [Hz]	50
Network impedance	Z_{net}	3,91
Network resistance	R_{net} [mΩ]	0,77
Network reactance	X_{net} [mΩ]	3,83

5.2   Transformer

The power rating of the transformer is selected by assuming the rated current on the secondary side of the transformer to be equal to the sum of rated currents of motors. Based on the rated currents, the nominal apparent power of the transformer is S_n = 1,6 MVA that is used the simulation.

When the nominal apparent power is known, typical transformer values can be found from the transformer catalogs or guidelines. For example, typical transformer`s rating plate values for 1,6 MVA - 2,5 MVA transformers are shown in Table 4.

Table 4. Transformer rating plate values. *(ABB, 2000)*

Transformer parameter		Rated value		
Nominal power	S_n [kVA]	1 600	2 000	2 500
Maximum no-load losses	P_0 [W]	1 840	2 130	2 550
Maximum load losses	P_k [W]	14 100	16 000	18 000
Short circuit impedance	z_k [%]	5,50	6,00	6,00
Zero sequence impedance	Z_0 [%]	5,70	6,40	6,40
No load current	I_0 [%]	0,40	0,30	0,30

Figure 33 shows the short circuit simulation`s equivalent circuit. Values for transformer parameters used in the simulation can be calculated based on the transformer`s rated values and are as listed in Table 5.
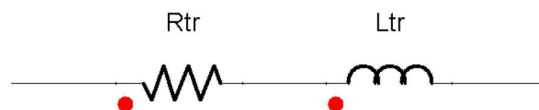
Figure 33. Simulation model of transformer

Table 5. Transformer values used in simulation.

Transformer parameter		Value		
Transformer apparent power	S_n [kVA]	1600	2000	2500
Transformer resistance	R_k [mΩ]	0,88	0,64	0,46
Transformer reactance	X_k [mΩ]	5,43	4,76	3,81

5.3 Fuse

Fuse is modeled in simulation as a voltage source, which is activated and set to arc voltage when the short circuit starts. In series with the voltage source are resistance and inductance of the fuse, as well as a switch representing the opening of the fuse. The components used for the fuse simulation are shown in Figure 34.

Figure 34. Fuse equivalent circuit used in simulation.

Fuses in simulation use the fuse i^2t values plotted in Figure 38 - Figure 40. These graphs were created based on the time current curves of fuses shown in Figure 35 - Figure 37. The time current curves were created using the values given in fuse manufacturer`s data sheets (Appendix 1-3). The simulation uses non-linear datasets for the fuse parameters and these datasets then give the i^2t-values as well as maximum permissible currents of fuses during the short circuit.
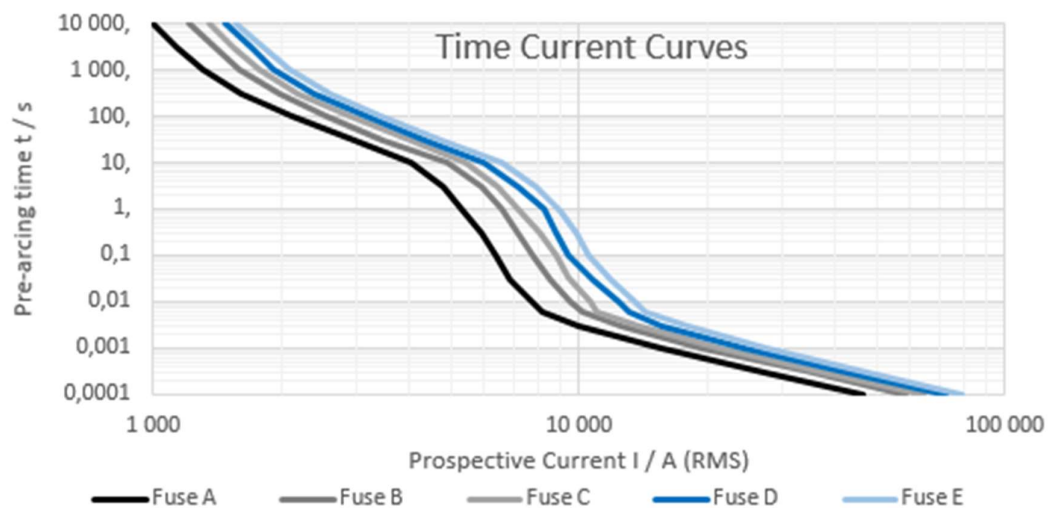
Figure 35. Fuse time current curves for fuse simulation. Fuses A–E
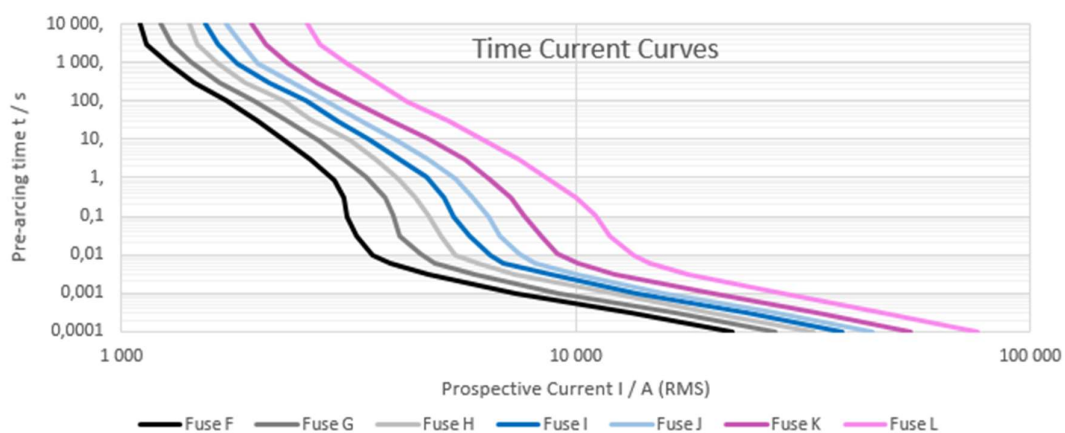
Figure 36. Fuse time current curves for fuse simulation. Fuses F–L
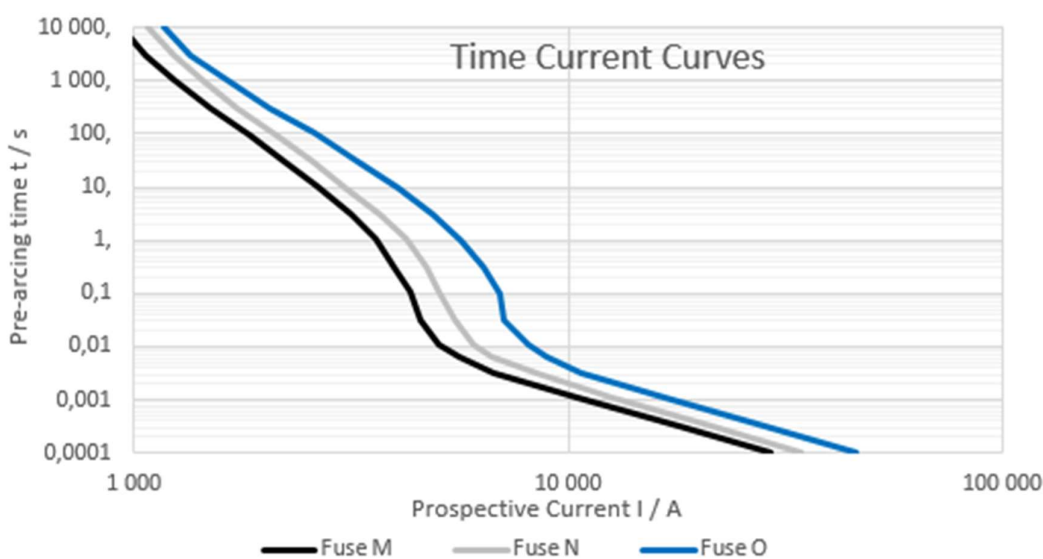
Figure 37. Fuse time current curves for fuse simulation. Fuses M–O
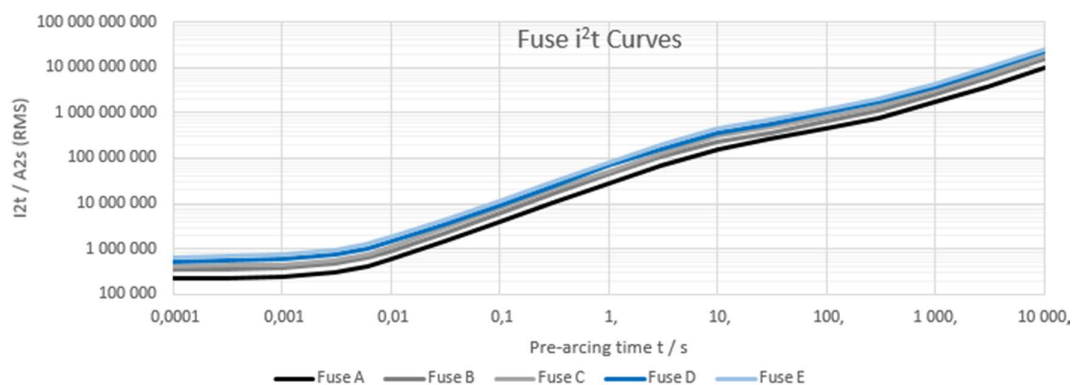
Figure 38. Fuse i²t curves. Fuses A–E
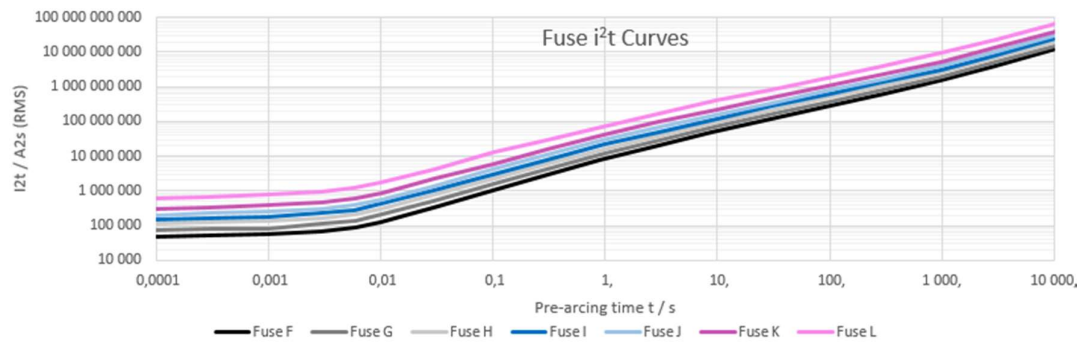
Figure 39. Fuse i²t curves. Fuses F–L
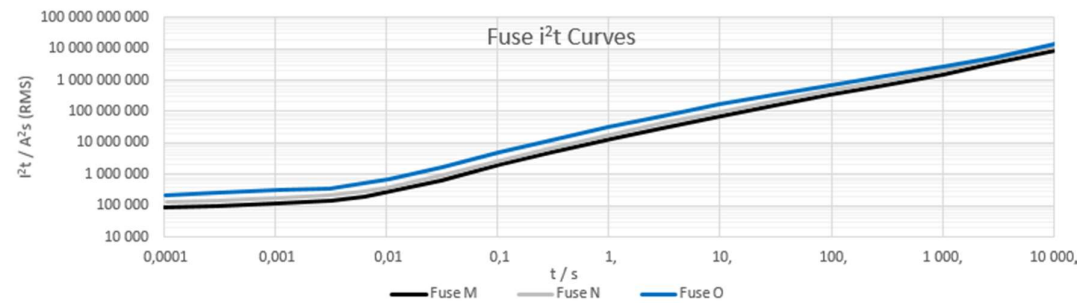
Figure 40. Fuse i²t curves. Fuses M–O

Fuse resistance is estimated based on power losses indicated in data sheets. Fuse power loss can be calculated using equation (24).

$$P_{Loss} = 3 \cdot I_{Rated}{}^2 \cdot R_{Fuse} \cdot cos\varphi \qquad (24)$$

When cos φ ≈1, the fuse resistance is calculated as a function of fuse power loss and rated current of the fuse. These values are shown in Table 6.

$$R_{Fuse} = \frac{P_{Loss}}{3 \cdot I_{Rated}{}^2}$$

Table 6. Fuse rated values

Fuse type	I_{Rated} [A]	P_{Loss} [W]	R_{Fuse} [µΩ]
Fuse A	1000	56	19
Fuse B	1250	61	13
Fuse C	1400	70	12
Fuse D	1500	72	11
Fuse E	1600	74	10
Fuse F	700	110	75
Fuse G	800	115	60
Fuse H	900	120	49

Fuse I	1000	125	42
Fuse J	1100	130	36
Fuse K	1250	140	30
Fuse L	1600	160	21
Fuse M	630	115	97
Fuse N	700	120	82
Fuse O	800	125	65

The values for fuse parameters are then estimated based on calculated fuse resistances and are as shown in Table 7. Inductance of the fuse is assumed to be insignificant in short circuit calculations and thus is not included in the simulation.

Table 7. Resistance and inductance parameters for fuse simulation

Fuse parameter	Value [mΩ]
R_{Fuse}	0,05
L_{Fuse}	-

The basic principle of the fuse operation is presented in Figure 41 and Figure 42. Fuse model compares the I^2 value of the fuse shown in Figure 41 at the given moment t with the current I^2 flowing in the circuit in Figure 42. The comparison starts at time t_1 when the current has risen over a predefined level I_1 and ends when current I_2 is below the limit at t_2. Fuse trips when the i^2t of the circuit reaches the i^2t limit of the fuse.
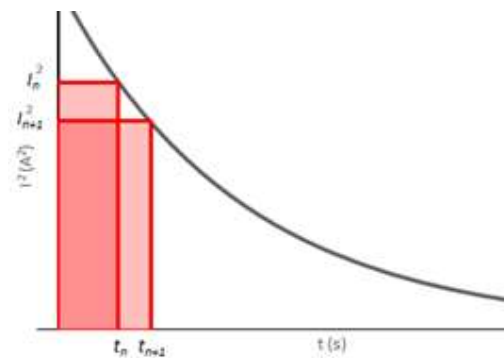
Figure 41. i^2t value of fuse as an area covered by current squared I^2 and time t
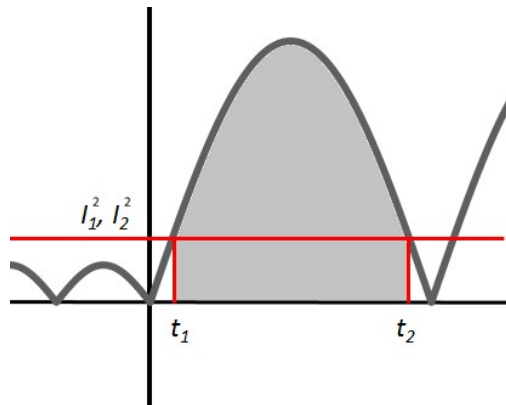
Figure 42. Total i²t value of current in circuit between t_1 and t_2

5.4 Rectifier

Rectifier circuit in the studied drive consists of three diodes and three thyristors. Both the diodes and the thyristors in diode-thyristor bridges in the simulation are modelled with diodes that have 0,8V forward voltage. Simulating the thyristors with diodes is sufficient for simulation purposes, because thyristors are needed during the charging of DC link capacitances, but don`t have much impact on short circuit currents of the system. Diode-thyristor bridge with RC Snubber circuit used in the simulation is shown in Figure 43.
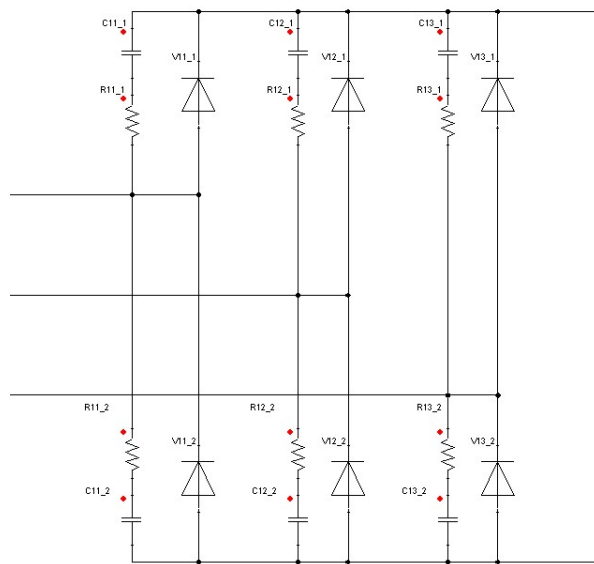
Figure 43. Simulation model of the diode-thyristor bridge.

Diodes and thyristors should be coordinated with the i²t and peak let-through current of the fuse (Appendix 4-6). Component breakdown values of semiconductor components are not included in the simulation, but the comparison of thyristor bridge i²t values with i²t values of fuses is done separately to check the durability of components during a short

circuit. A component is protected against short circuit when let-through currents of fuse and fuse clearing times are less than the component withstand ratings. Semiconductor surge current withstand is usually published in terms of half cycle current rating and the duration is 8,33 ms or 10 ms depending on supply frequency of 50 Hz or 60 Hz. Also, peak arc voltages of fuses are compared to the values given in semiconductor data sheets. Figure 44 shows the peak arc voltages of fuses as a function of the applied voltage level in RMS.
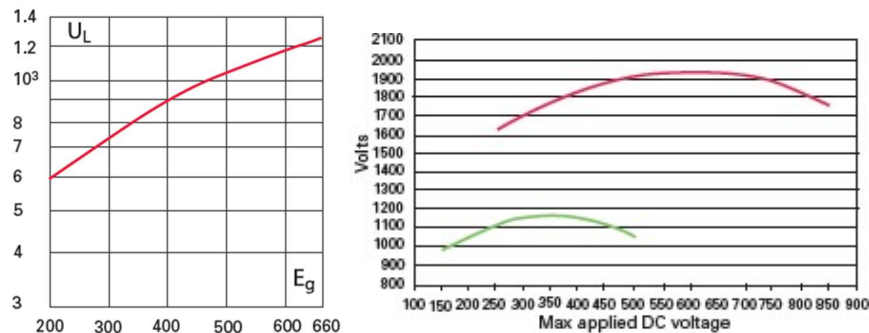
Figure 44. Peak arc voltages of fuses for semiconductor coordination. (Eaton, 2016, pp. 11, 24)

Table 8 - Table 11 shows the comparison of thyristor i^2t and fuse i^2t values, as well as fuse operating times required for sufficient thyristor protection.

Table 8. Comparison of thyristor i^2t and AC fuse i^2t values.

AC Fuse	Fuse minimum pre-arcing i^2t [A²s]	Fuse Clearing i^2t [A²s]	Thyristor	Thyristor i^2t [A²s]
Fuse B	300 000	2 150 000	Thyristor A	1 050 000
Fuse E	585 000	4 150 000	Thyristor A	1 050 000
Fuse B	300 000	2 150 000	Thyristor B	1 201 250
Fuse C	380 000	2 700 000	Thyristor B	1 201 250
Fuse D	470 000	3 350 000	Thyristor B	1 201 250
Fuse E	585 000	4 150 000	Thyristor C	1 201 250
Fuse A	140 000	985 000	Thyristor D	320 000

Table 9. Required fuse operation times of AC fuses for thyristor protection.

AC Fuse	Thyristor i^2t [A²s]	AC Fuse time [ms]
Fuse B	1 050 000	10-15
Fuse E	1 050 000	3-4
Fuse B	1 201 250	10-20
Fuse C	1 201 250	10-15

Fuse D	1 201 250	7-9
Fuse E	1 201 250	5-6
Fuse A	320 000	3-4

Table 10. Comparison of thyristor i²t and DC fuse i²t values.

DC Fuse	Fuse minimum pre-arcing i²t [A²s]	Fuse Clearing i²t [A²s]	Thyristor	Thyristor i²t [A²s]
Fuse I	140 000	945 000	Thyristor A	1 050 000
Fuse K	290 000	1 950 000	Thyristor A	1 050 000
Fuse L	580 000	3 900 000	Thyristor B	1 201 250
Fuse G	69 500	465 000	Thyristor B	1 201 250
Fuse H	100 000	670 000	Thyristor B	1 201 250
Fuse K	290 000	1 950 000	Thyristor C	1 201 250
Fuse F	44 500	300 000	Thyristor D	320 000

Table 11. Required fuse operation times of DC fuses for thyristor protection.

DC Fuse	Thyristor i²t [A²s]	DC Fuse time [ms]
Fuse I	1 050 000	30-35
Fuse K	1 050 000	10-15
Fuse L	1 201 250	5-6
Fuse G	1 201 250	40-70
Fuse H	1 201 250	30-50
Fuse K	1 201 250	15-25
Fuse F	320 000	27-30

5.5 AC Choke

AC choke equivalent circuit in the simulation model shown in Figure 45 has constant resistance and non-linear inductance. The non-linear inductance represents the change in choke behaviour with high currents when the choke saturates.
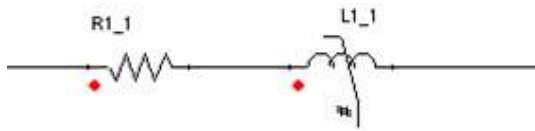
Figure 45. Simulation model of AC Choke

AC choke inductance curves have been estimated based on saturation measurements. In cases where the test results are insufficient, the saturation curves are extrapolated

based on the expected results. Extrapolation is based on the theory of how chokes should behave with high currents and also to the measured values of other similar chokes.

Figure 46-Figure 51 show the measured phase inductances in dotted lines as well as the non-linear inductance in red continuous line that is used in simulations. Inductances are plotted as a function of current. In the simulation, it is assumed that the inductance stays constant after reaching the minimum inductance value during the saturation when the ferromagnetic core starts to behave like an air core.
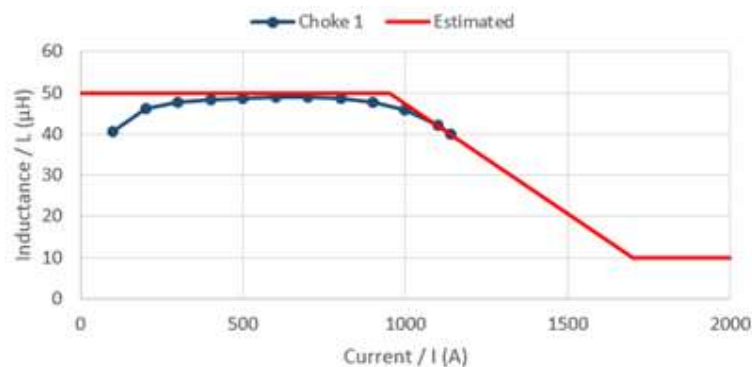
Figure 46. Non-linear inductance of choke A in simulation
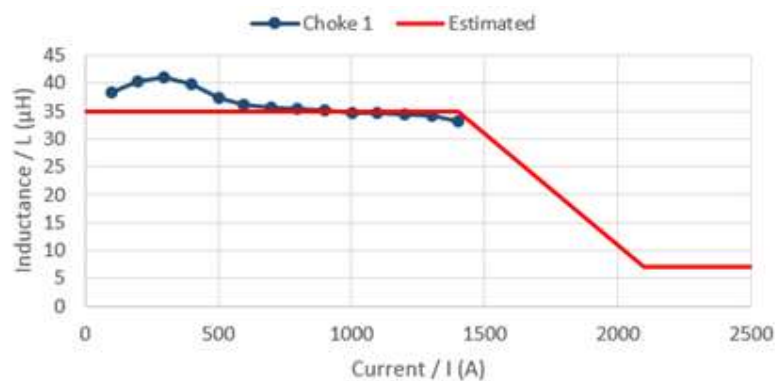
Figure 47. Non-linear inductance of choke B in simulation
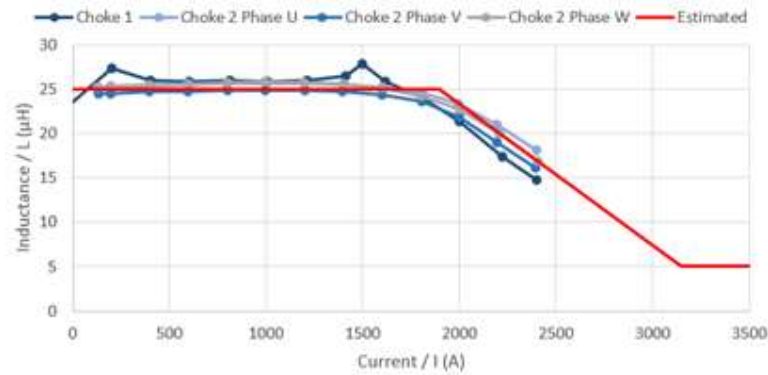
Figure 48. Non-linear inductance of choke C in simulation
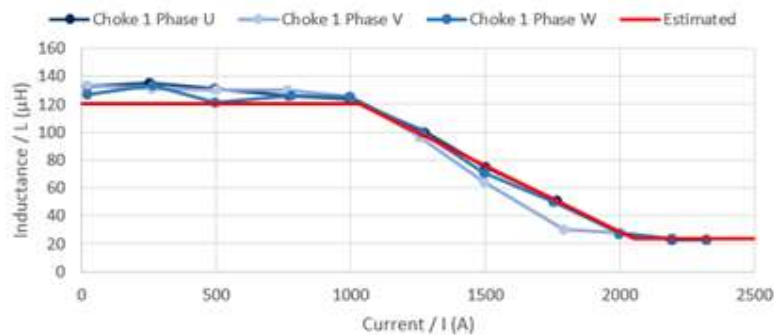
Figure 49. Non-linear inductance of choke D in simulation
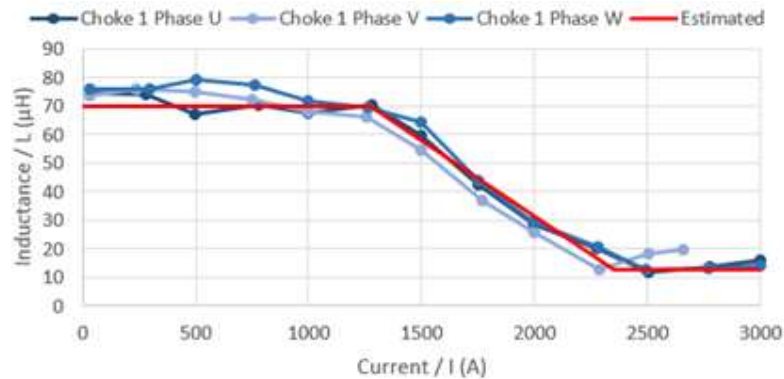
Figure 50. Non-linear inductance of choke E in simulation
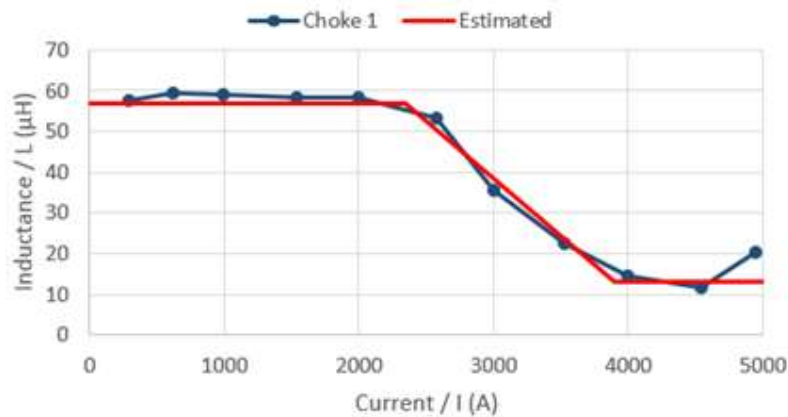
Figure 51. Non-linear inductance of choke F in simulation

Based on the non-linear curves for inductances, the choke parameters nominal peak current I_N, nominal inductance L_N and saturation current I_{min} and saturation inductance L_{min} can be estimated and are as shown in Table 12.

Table 12. AC choke resistance and non-linear inductance.

Type	R_Choke [mΩ]	I_N [A]	I_{min} [A]	L_N [µH]	L_{min} [µH]
Choke A	0,87	950	1700	50	10
Choke B	0,73	1400	2100	35	7
Choke C	0,54	1900	3150	25	5
Choke D	2,09	1030	2050	120	24
Choke E	1,46	1275	2350	70	13
Choke F	1,23	2350	3900	57	13

5.6   Inverter

When estimating the AC or the DC short circuit currents in the supply side of the inverter, the inverter itself doesn`t have a large contribution except for the DC capacitors, which causes high current peaks immediately after the shot circuit. Because detailed modeling of an inverter is also much more difficult, the simulation simplifies the inverters as capacitors with series resistance ESR (Equivalent series resistance) and series inductance ESL (Equivalent series inductance) Equivalent circuit used in simulations is shown in Figure 52.
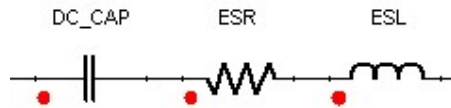
Figure 52. Equivalent circuit of DC link capacitor with series resistance and capacitance.

Capacitance values of inverters for the simulations are the same as given in drive manuals. ESR and ESL values of inverter capacitors are obtained from the capacitor data sheets. The value for the series resistance for simulations is the average of values given in data sheet for ESR between 20 degrees and 70 degrees in 3 kHz frequency. The values for capacitance, series resistance and series inductance are listed in Table 13.

Table 13. DC link capacitor values.

DC Capacitance [mΩ]	ESR [mΩ]	ESL [µΩ]
4,7	4,5	0,63
9,3	4,5	0,63
14	4,5	0,63
21	4,5	0,63

5.7   Conductors

Simulations include the supply and motor cables as well as the conductors for the components and for the DC link. Cables are modeled in simulations using resistors and inductances in series as shown in Figure 53. Cable dimensioning and the number of cables are based on nominal current values (Appendix 7-10) and conductor lengths have been estimated for the typical drive configuration. When the cable length is increased, the impedance in the circuit also increases, so the short circuit values are highest when the cables are short.

Figure 53. Cable impedance in simulation model

In the simulation, only cables are used. This is because simulating busbars can be more complex and sufficient accuracy for the short circuit purposes can be achieved when the conductors are assumed to be cables. Resistances and inductances of the cables are based on cable data sheets. Cable impedance values at conductor temperature 20 °C

and rated frequency are used according to the IEC standard 61363-1. The impedance caused by the cabling is however relatively small compared to the total impedance of the circuit, so sufficient accuracy is achieved by using average values for cable impedances. Resistance and reactance values of cables used in the simulation model are shown in Table 14.

Table 14. Cable resistance and reactance.

Cable parameters	Value [mΩ / m]
R_Cable	0,05
X_Cable	0,04

5.8 Motor Load

In case of short circuit, the motor begins to function as a generator and feeds the fault with energy, which is stored in the magnetic circuit of the motor. A numerical value of the motor contribution can be calculated by a subtransient reactance X, which is an electrical representation of the motor. The subtransient reactance is, however, usually difficult to find, therefore motor contribution as a multiple of the rated current of the motor gives usually correct values within sufficient accuracy. (ABB SACE, 2017, p. 69)

The effect of the motor in simulations has been estimated by comparing no load values of the short circuit to the values with the motor contribution, which feed the current to the short circuit. Table 15 shows the values used in simulations and the motor equivalent circuit is shown in Figure 54.
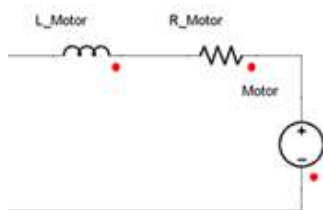
Figure 54. Motor load in short circuit simulation model.

Table 15. Motor parameters.

Motor contribution	Motor resistance	Motor inductance
$I = 6 \cdot I_{n\_motor}$	R_motor = 50 mΩ	L_motor = 3 mH

6 Simulation Cases

The study focuses on finding the optimal DC link protection method by comparing different fuse arrangements in the DC link. Several different simulation cases were studied, each with either two fuses, six fuses or eight fuses in a configuration shown in Figure 55:

1. Two DC fuses, DC fuses between two module pairs
2. Six DC fuses, DC fuses between each module
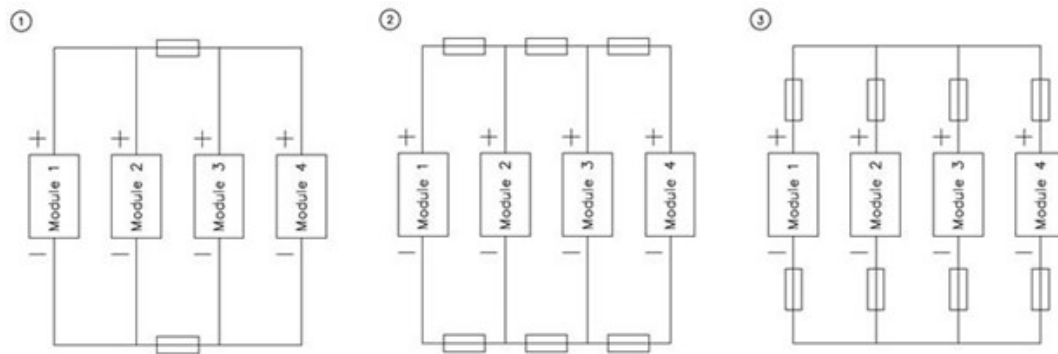3. Eight DC fuses, DC fuses for each module

Figure 55. DC fuse configurations with two, six or eight fuses

The benefit of increasing the number of fuses is to decrease the duration of the short circuit by faster fuse operating times, which in short circuit circumstances can significantly reduce the damage to the components. However, increasing the number of fuses requires more space for the drive cabinet and also increases the component costs of the drive. That is why there should be a clear benefit from having more fuses.

The simulation components described in the previous chapter were arranged so that the drive system consists of in total of four parallel drive modules that have a common DC link as shown in Figure 56. Simulations were done with both 6-pulse and 12-pulse connection to study if the short circuit behavior changes between the two configurations.
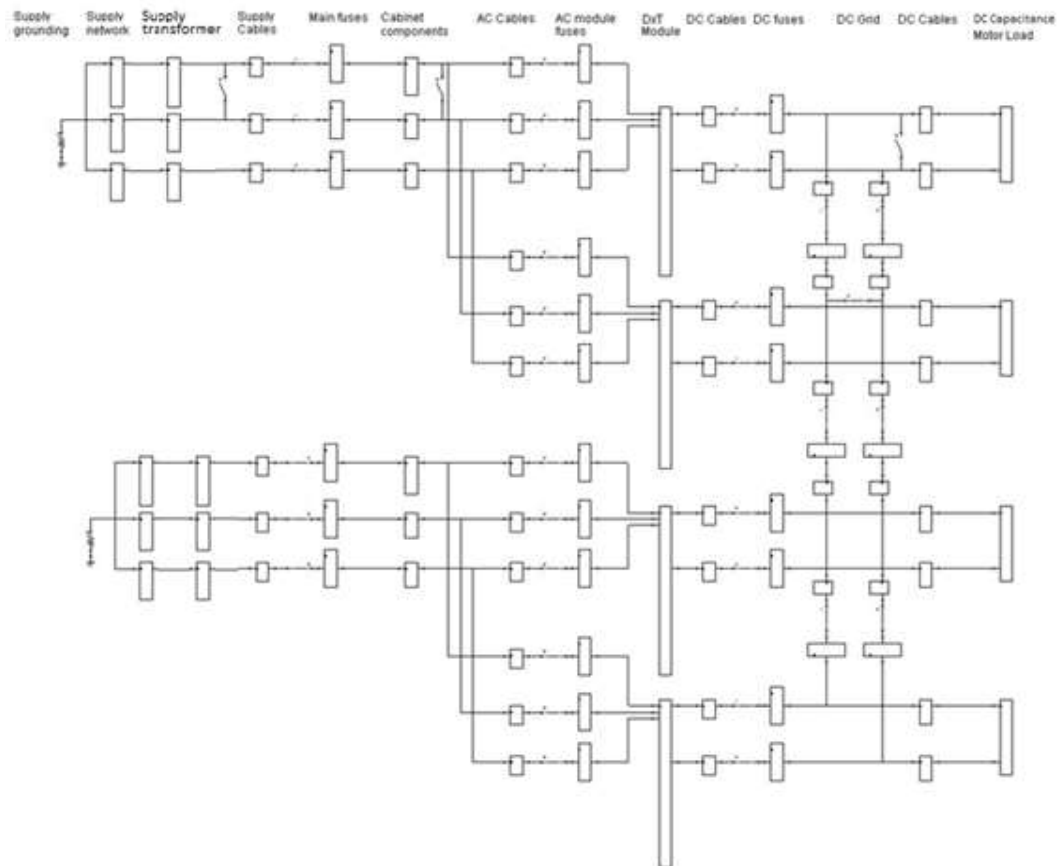
Figure 56. Simulation model of AC Drive system

Configurations with two, six and eight fuses where then simulated in five different simulation cases shown below in Figure 57 - Figure 61. The cases 1 and 2 were done with two parallel drive modules and the cases 3-5 have four parallel drive modules. By comparing the short circuit currents with two and four parallel drive modules, it can be seen what kind of effect increasing the number of parallel modules has on maximum short circuit currents as well as on the operating times of fuses.

In simulation case 1 there are two parallel connected modules with no DC fuses between the modules and in case 2 there are two fuses between the modules. In simulation cases with four parallel modules, there are two fuses between the modules in case 3, six fuses between the modules in case 4 and a total of eight fuses after each module in case 5. Simulation cases differ only by the amount of parallel connected modules as well as by the configuration and amount of fuses. The short circuit point is in each case at the end of the DC link, which is estimated to be the most difficult from the protection point of view.

Otherwise, the drive system parameters are the same and there are no differences be-tween the circuits. It is also assumed that the short circuit conditions don`t change during the short circuit for example because of new short circuit connections caused by heavy forces.

Simulation case 1: Short Circuit at the end of DC connection busbars of two parallel connected modules with no DC fuses, 6-pulse and 12-pulse. (Figure 57)
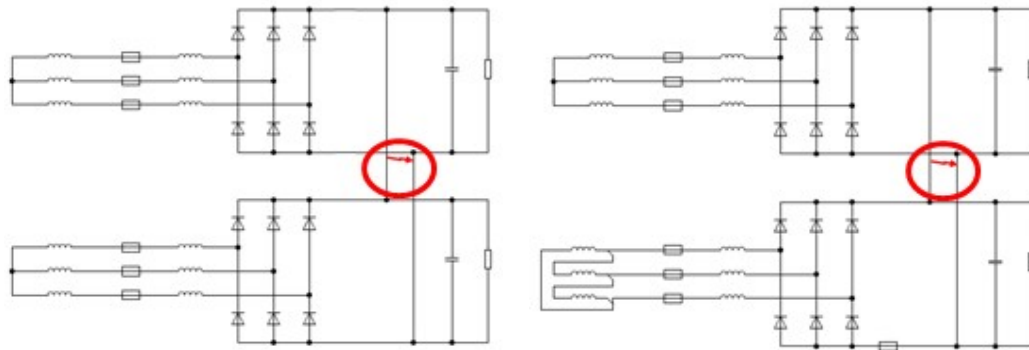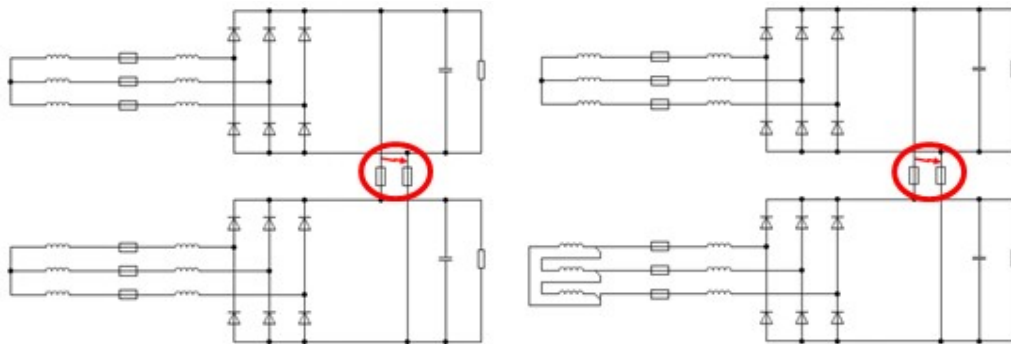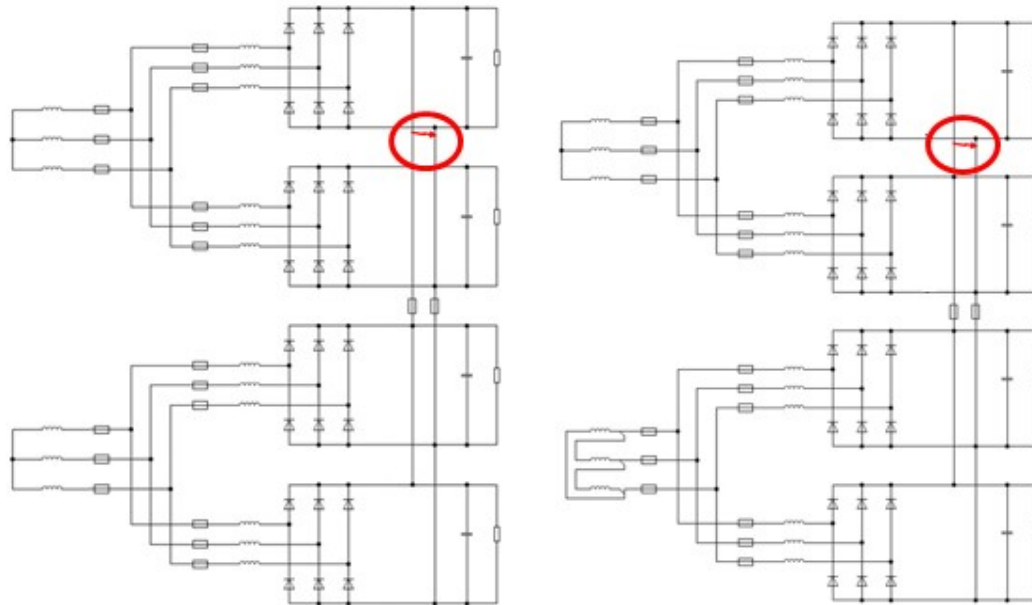

Figure 57. Case 1. Two parallel connected modules with no DC fuses. 6-pulse and 12-pulse connection.

Simulation case 2: Short Circuit at the end of DC connection busbars of two parallel connected modules with two DC fuses between drive modules, 6-pulse and 12-pulse (Figure 58)

Figure 58. Case 2. Two parallel connected modules with DC fuses. 6-pulse and 12-pulse connection.

Simulation case 3: Short Circuit at the end of DC connection busbars of four parallel connected modules with two DC fuses, 6-pulse and 12-pulse. (Figure 59)

Figure 59. Case 3. Four parallel connected modules with two DC link fuses. 6-pulse and 12-pulse connection.

Simulation case 4: Short Circuit at the end of DC connection busbars of four parallel connected modules with six DC fuses, 6-pulse and 12-pulse (Figure 60)
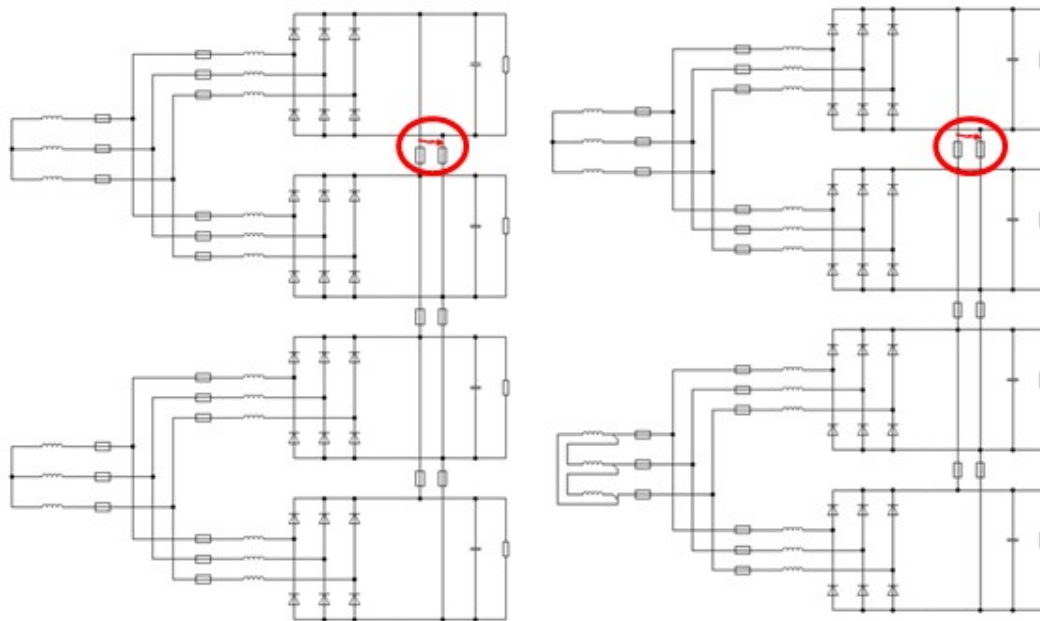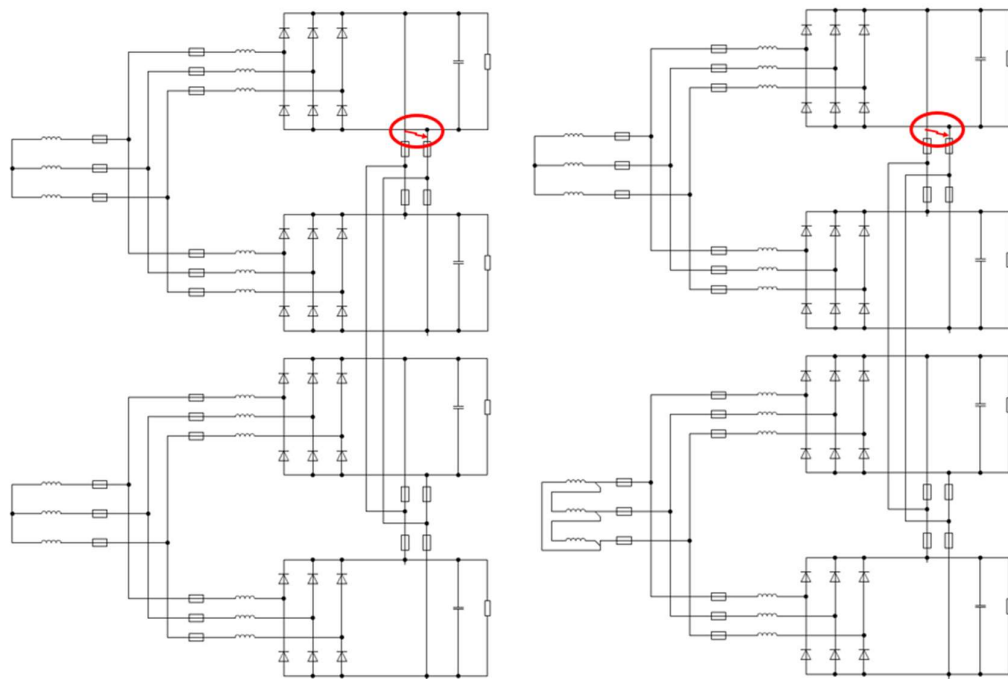

Figure 60. Case 4. Four parallel connected modules with six DC link fuses. 6-pulse and 12-pulse connection.

Simulation case 5: Short Circuit at the end of DC connection busbars of four parallel connected modules with eight DC fuses, 6-pulse and 12-pulse (Figure 60)

Figure 61. Case 5. Four parallel connected modules with eight DC module fuses. 6-pulse and 12-pulse connection.

7   Simulation Results

Current share in normal operating conditions compared to the nominal load values was shown in the previous chapter in Figure 31. It can be seen from Figure 62 that current share in normal operation with even current distribution, the current in DC link between two outermost modules is about a fifth of the load current and the current in the middle of the DC link is twice the current at about 40 % of the load. Respectively, compared to the supply values, the currents in the DC circuit are a bit less than one third and two thirds of the AC supply current.
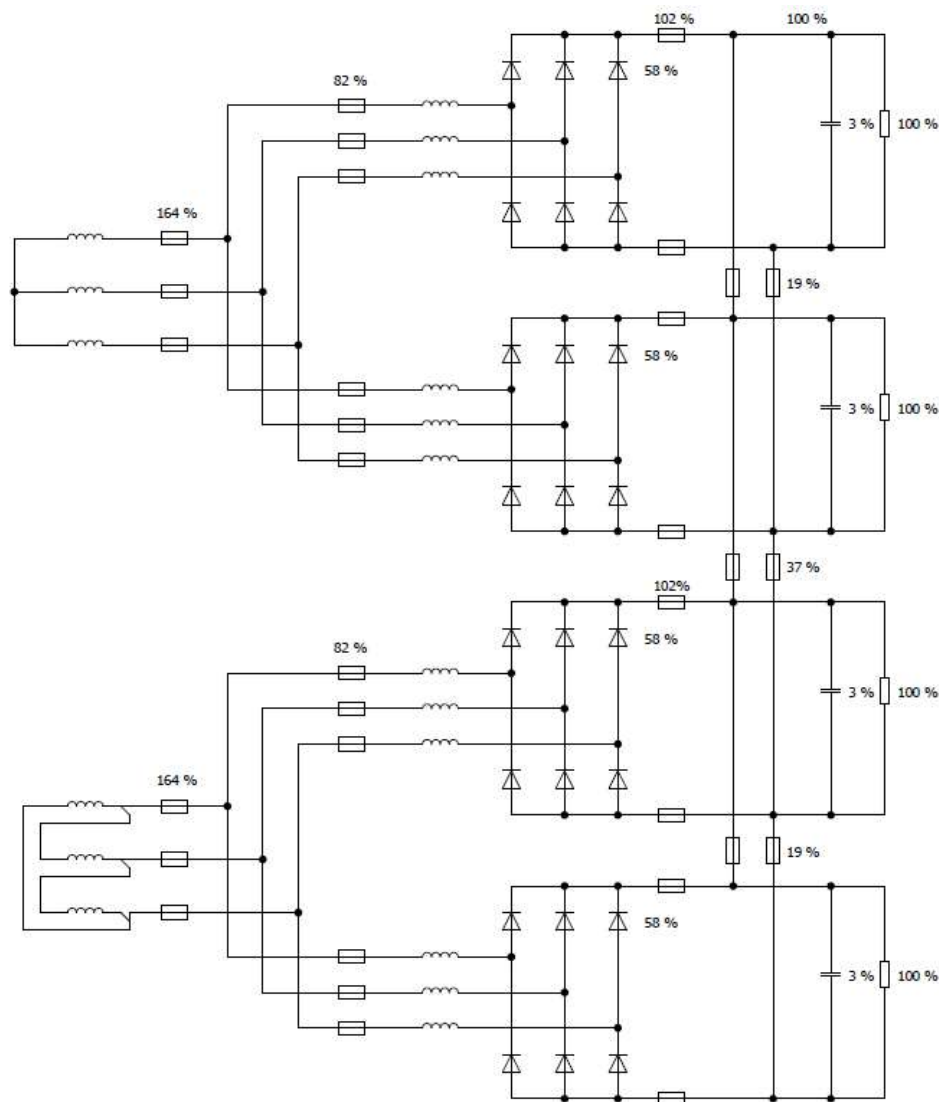
Figure 62. Current share with four modules connected in parallel

In Figure 63 is an example of simulation showing current in the circuit compared to the fuse operating values in percentages. Figure shows which of the fuses operate during short circuit, as well as the operating times of fuses. Because current rises very steeply right after the fault, in some conditions more than one fuse may operate according to the simulations.
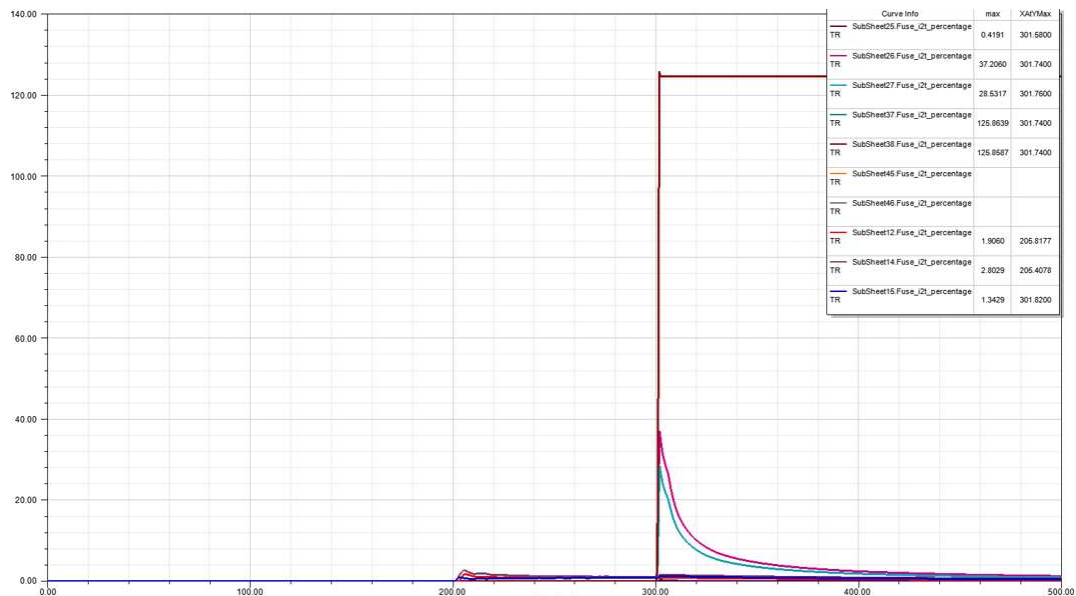

Figure 63. Fuse operation during short circuit

Even though the main goal of the study was to find the best method for DC link protection, the reliability of the simulation model was first tested with other configurations. In Table 16, the AC and DC short circuit values have been tested with one, two and four parallel connected module with both 6-pulse and 12-pulse configurations. Each module has main fuses and DC fuses after the rectifier circuit. For each configuration, maximum AC short circuit current values were collected before main fuses operated and also DC short circuit currents for DC fuses respectively. In addition, each measurement was done with a load, and without the load, to see the effect of motors in the circuit.

It can be seen that the AC short circuit currents are very close to each other in each case. This means that the AC fuses operate in similar time scales in each configuration. It can also be seen from the results that the 6-pulse and 12-pulse configurations give

similar results. Also, the results show that the effect of load on the short circuit is not significant.

Table 16. Short circuit in main supply with different configurations.

Modules	Pulses	Current with main fuses [kA]		Current with DC fuses [kA]	
		With load	No Load	With load	No Load
1	6-p	43,7	43,6	37,5	37,5
2	6-p	43,7	43,7	22,0	22,0
2	12-p	43,7	43,7	22,0	22,0
4	6-p	43,7	36,2	11,1	13,7
4	12-p	43,8	43,7	11,0	13,7

Short circuit in the DC link of four parallel connected drive modules was tested with two, six and eight fuses. These results correspond to the cases 3-5 shown in Figure 59 - Figure 61. Maximum short circuit currents and fuse operating times are shown in Table 17 for 6-pulse and in Table 18 for 12-pulse configuration.

The results show that the difference between operating times of two, six and eight DC fuses is quite small and in each case, the fuse operation is very fast. In the case of two fuses, the operating time is longer, although it`s nevertheless sufficiently fast for protecting the components in the circuit. Slower operating time is caused by the longer distance from the short circuit location to the fuses. Also, the maximum short circuit currents are higher compared to the six fuse and eight fuse protection methods. It can be also seen from the results that the effect of load or the pulse number of supply doesn`t have a significant effect on results. Based on simulations, each of the three fuse solutions should provide sufficient protection for the short circuit.

Table 17. Short circuit values with 4 parallel modules and 6-pulse configuration

	With load [kA]	Time [ms]	No Load [kA]	Time [ms]
Two fuses	67,6	0,34	67,9	0,32
Six fuses	57,3	0,26	56,8	0,26
Eight fuses	34,1	0,26	33,6	0,25

Table 18. Short circuit values with 4 parallel modules and 12-pulse configuration

	With load [kA]	Time [ms]	No Load [kA]	Time [ms]
Two fuses	67,9	0,33	67,5	0,32
Six fuses	56,8	0,28	56,3	0,25
Eight fuses	34,3	0,28	34,0	0,25

7.1   Simulation Accuracy

Short circuits are extreme and sudden conditions, which causes more uncertainties to the results compared to simulations done for normal operation of the drive. Many of the components in the circuit can behave differently in short circuit conditions than in normal operation. Even though these variations have been considered during the study, the actual values during the short circuit can differ from the simulated values.

The drive system from supply to load contains a large number of components. To prevent the simulation model to become too complex and slow, some of the components have been simplified, which increases the error margin for the results. These components include the inverters and the motors. For example, if the short circuit begins with a full load, the motor can cause additional current flow towards the faulted circuit. In this study, only the basic motor model was used and improving the simulation model of the motor could give more accurate results. These components, however, shouldn`t have a big impact on short circuit currents or fuse operating times in DC link short circuit, so the simpler representation can be reasoned.

The reliability of the simulations was estimated by making simulations also in normal operation and by comparing short circuit values in different parts of the circuit and with different drive configurations. By comparing the results of simpler short circuit cases to typical short circuit values, the accuracy and reliability of results were increased.

8   Conclusions

The fuse is considered to be current limiting when it operates before the current reaches its maximum unrestricted values. This requirement was reached with all three fuse solutions that were studied and the necessary i^2t energies were quickly exceeded well before the current would reach its maximum values. This by itself doesn`t mean that the requirements assigned to the fuses are fulfilled. The first priority for fuse protection is safety. This typically means that the minimum requirement is that the damages caused by the short circuit should always be limited to the drive cabinet and the failure shouldn`t have an effect on the other parts of the system. Ideally, the short circuit protection would also prevent drive components from extensive damage. Often the real situation can be between these two cases. The protection prevents short circuit currents from spreading other parts of the system, but the short circuit can cause damage to components such as semiconductors, even with very fast fuse operating times.

To achieve sufficient protection, both the mechanical and thermal effects of the short circuit should be minimized. The mechanical forces are caused by maximum let through current values and these forces can result in deformation of components, as well as high mechanical stresses to insulators. Thermal effects are caused by the I^2t energy values as a combination of RMS let-through current and clearing time of the fault. A sudden thermal impact caused by the short circuit weakens the insulation and increases the aging of the components, which can affect the component properties and also further reduce the mechanical strength of the system. These forces combined can lead from phase to phase fault to a three-phase short circuit and cause considerable damage to the system if the short circuit is not interrupted quickly.

Based on the results, having six or eight fuses in the DC link would not give a clear benefit compared to the solution with two fuses when short circuit currents and fuse operating times are compared. So from the safety and component protection point of view having two fuses is sufficient, based on simulations. Similar kinds of results have been obtained also from other analyses, which further supports these results.

When considering protection concept for the whole drive system, the user and system requirements should also be taken into account. Even if two fuses in the DC link can protect expensive and vulnerable drive components, adding more fuses to the DC link can offer other kinds of benefits, such as better isolation of the faulty part of the drive

from the short circuit. This would allow that at least some parts of the drive could continue operation right after the short circuit.

In this study, it was assumed that from the protection point of view the most challenging case is when the short circuit occurs at the end of the DC link. A short circuit can result from various other reasons, such as the fault caused by semiconductors or DC capacitors and the likelihood of these events as well as the impact to the drive can be considered when protection concept is planned for the drive system.

However, even during the short time period, the short circuit currents reaches high values that could potentially cause damage to the components. Simulation parameters, such as short circuit impedance, can have a big impact on the resulting short circuit currents. Because of the uncertainties of the simulation, also other methods to verify the actual fuse operation during the short circuit may be needed. Short-circuit calculations and testing are an important part of the component selection and should be done whenever possible.

The simulation model was optimized for examining the behaviour of the circuit for the first few cycles after the initialization of short circuit, which is sufficient when examining the maximum current and operating times of fuses during short circuit during pre-arcing phases. This makes it difficult to estimate the component durability during a short circuit. In future studies, the simulation model could be optimized and extended for longer durations after the initiation of a short circuit. This would mean for instance that the fuse simulation models could be optimized to better take into account the total arcing times instead of pre-arcing time. Knowing the total i^2t energy with sufficient accuracy would improve the estimations of the component durability during a short circuit.

Effect of unbalances in the network can have an effect on the current distribution in the circuit and for example, the DC capacitors can have high tolerances in the capacitance values. Also, the transformer selection can have a high impact on the network in the secondary side of the transformer. In this study, these variations were not taken into account except for the generic correction factors. In later studies, the effects of these tolerances could be estimated in more detail to get more accurate values for the selection of the protective device.

9   References

ABB. (2000). *TTT-käsikirja, Chapter 11: Tehomuuntajat.*

ABB. (2010). *Transformer handbook.*

ABB. (2010). *XLPE Land Cable Systems User´s Guide.* Retrieved from
https://library.e.abb.com/public/ab02245fb5b5ec41c12575c4004a76d0/XLPE%
20Land%20Cable%20Systems%202GM5007GB%20rev%205.pdf

ABB Drives. (2009). *Reducing harmonics caused by variable speed drives.* Retrieved
from
https://library.e.abb.com/public/afa9690deb15a092c125744f003cb018/TD2_Re
ducing_harmonics_EN_revD_LR.pdf

ABB Drives. (2011). *Technical guide No. 4, Guide to variable speed drives.*

ABB Drives. (2011). *Technical guide No. 8, Electrical braking.*

ABB Drives. (2015). Hardware manual, ACS880-304 +A018 diode supply modules.
(Revision C).

ABB Drives. (2017). Application guide, ACS880-01 drives and ACS880-04 drive
modules, Common DC systems. (Revision C).

ABB Drives. (2017). Hardware manual, ACS880-04XT drive module packages (500 to
1200 kW). (Revision D).

ABB Drives. (2017). *Supplement ACS880-04XT drive module packages (1000 to 2400
kW).*

ABB Drives. (2017). *Technical guide No. 6, Guide to harmonics with AC drives.*

ABB Drives. (2018). *What is an AC drive*. Retrieved 5 18, 2018, from
http://new.abb.com/drives/what-is-a-drive

ABB Low Voltage Switches. (2004). Fusegear, DIN-type HRC-fuse links, 2...1600 A
gG- and aM- types.

ABB SACE. (2011). Technical Application Papers No. 5. ABB circuit-breakers for direct
current applications.

ABB SACE. (2015). *Technical Application Papers No. 14. Faults in LVDC microgrids
with front-end converters.*

ABB SACE. (2017). *Technical Application Papers No. 15, The MV/LV transformer
substations (passive users).*

ABB SACE. (2017). *Technical Application Papers No. 24, Medium voltage direct
current applications.*

AEMO. (n.d.). *Fact sheet: System strength*. Retrieved from https://aemo.com.au/-
/media/Files/Electricity/NEM/Security_and_Reliability/Reports/2016/AEMO-
Fact-Sheet-System-Strength-Final-20.pdf

Broussard, D. (2013). *Understanding short circuit motor contribution.* Retrieved from

    http://apps.geindustrial.com/publibrary/checkout/SC-

    Motor?TNR=White%20Papers|SC-Motor|generic

Danfoss. (2014, 12). Facts Worth Knowing about Frequency Converters.

Eaton. (2007). Fuseology, Cooper Bussmann presentation.

Eaton. (2016). *High speed fuses applications guide.* Retrieved 11 24, 2017, from

    http://www1.cooperbussmann.com/pdf/9a13f527-0f4c-4e23-a060-

    b2e881a176f3.pdf

Eaton. (2016). *Protecting semiconductors with high speed fuses.* Retrieved from

    http://www.cooperindustries.com/content/dam/public/bussmann/Electrical/Reso

    urces/technical-literature/bus-ele-an-10507-hsf.pdf

Eaton. (2017). *Bussmann series full line catalog 1007.* Retrieved 11 25, 2017, from

    http://www.cooperindustries.com/content/dam/public/bussmann/Electrical/Reso

    urces/Catalogs/bus-ele-cat-1007-flc-2017-complete.pdf

Electronic Power Conversion, Line-Frequency Diode Rectifiers. (n.d.). Retrieved from

    https://ocw.tudelft.nl/wp-content/uploads/4._Diode_Rectifiers.pdf

Energiateollisuus. (2014). *Sähköntoimituksen laatu- ja toimitustapavirheen*

    sovellusohje. Retrieved from

    https://energia.fi/files/881/Sahkontoimituksen_laatu_ja_toimitustapavirheen_sov

    ellusohje_2014.pdf

Hammond Power Solutions Inc. (n.d.). *Transformers, Harmonic Currents and Phase*

    Shifting. Retrieved from

    http://www.hammondpowersolutions.com/files/HPS_article_Harmonics_PhaseS

    hifting.pdf

Hietalahti, L. (2013). *Sähkövoimatekniikan perusteet.* Vantaa: Tammertekniikka.

Hurley, W., & Wölfle, W. (2013). *Transformers and inductors for power electronics.*

    New York: Wiley.

International Electrotechnical commission. (1997). IEC 61660-1. Short-circuit currents

    in d.c. auxiliary installation in power plants and substations – Part 1: Calculation

    of short-circuit currents.

International Electrotechnical commission. (1998). *IEC 61363-1. Electrical installations*

    of ships and mobile and fixed offshore units – Part 1: Procedures for calculating

    short circuit currents in three-phase a.c.

International Electrotechnical commission. (2000). *IEC 60909-4. Short-circuit currents*

    in three-phase a.c. systems – Part 4: Examples for the calculation of short-
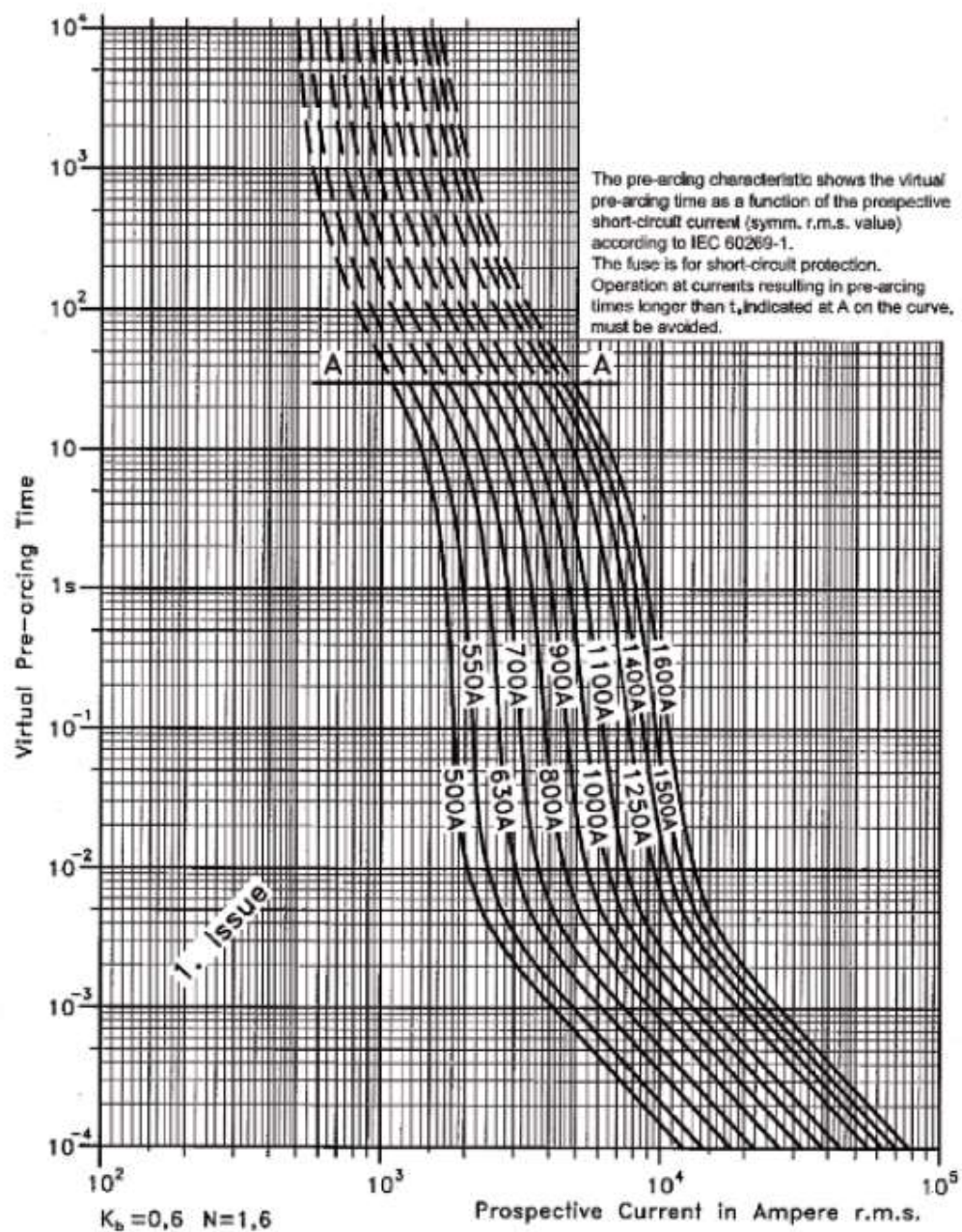
    circuit currents.

International Electrotechnical commission. (2002). *IEC 60909-1. Short-circuit currents in three-phase a.c. systems – Part 1: Factors for the calculation of short-circuit currents according to IEC 60909-0.*

International Electrotechnical commission. (2008). *IEC 60909-2. Short-circuit currents in three-phase a.c. systems – Part 2: Data of electrical equipment for short-circuit current calculations.*

International Electrotechnical commission. (2009). *IEC 60364-5-52. Low-voltage electrical installations – Part 5-52: Selection and erection of electrical equipment – Wiring systems.*

International Electrotechnical commission. (2016). *IEC 60909-0. Short-circuit currents in three-phase a.c. systems – Part 0: Calculation of currents.*

Markiewicz, H., & Klajn, A. (2004). *Power Quality Application Guide, Standard EN 50160 - Voltage Characteristics in Public Distribution Systems.* Retrieved from http://www.cdtechnics.be/542-standard-en-50160-voltage-characteristics-in.pdf

Mersen. (2011). *Semiconductor fuse applications guide.* Retrieved 11 25, 2017, from http://ep-us.mersen.com/fileadmin/catalog/Literature/Brochures/BR-Semiconductor-Fuse-Applications-Guide-Brochure.pdf

Mersen. (n.d.). *Application information.* Retrieved 11 24, 2017, from http://ep-us.mersen.com/uploads/Advisor/Advisor111-P-Applications-web.pdf

Schlabbach, J. (2005). *Short-circuit Currents, IET Power and Energy Series 51.* London: The institution of Engineering and Technology.

Silvonen, K. (2009). *Sähkötekniikka ja piiriteoria.*

Solbakken, Y. (2017, 5 1). *Switchcraft, Space Vector PWM Intro*. Retrieved from https://www.switchcraft.org/learning/2017/3/15/space-vector-pwm-intro

Tabrizi, M. (2015). *Integration of renewable energy sources: Strong challenge for a weak grid.* Retrieved from https://blogs.dnvgl.com/energy/integration-of-renewable-energy-sources-strong-challenge-for-a-weak-grid

The Institute of Electrical and Electronics Engineers. (1991). *AC/DC system strength as indicated by short circuit ratios.*

The Institute of Electrical and Electronics Engineers. (2005). *IEEE Std C37.010-1999. IEEE Application Guide for AC High-Voltage Circuit Breakers Rated on a Symmetrical Current Basis.*

UNLV College of Engineering. (n.d.). *Magnetic circuits.* Retrieved from http://www.egr.unlv.edu/~eebag/EE%20340%20-%20Magnetic%20Circuits.pdf

Wang, Z., & Lemmon, M. (n.d.). *Voltage and Frequency Stability of Weak Power Distribution Net-works with Droop-Controlled Rotational and Electronic*

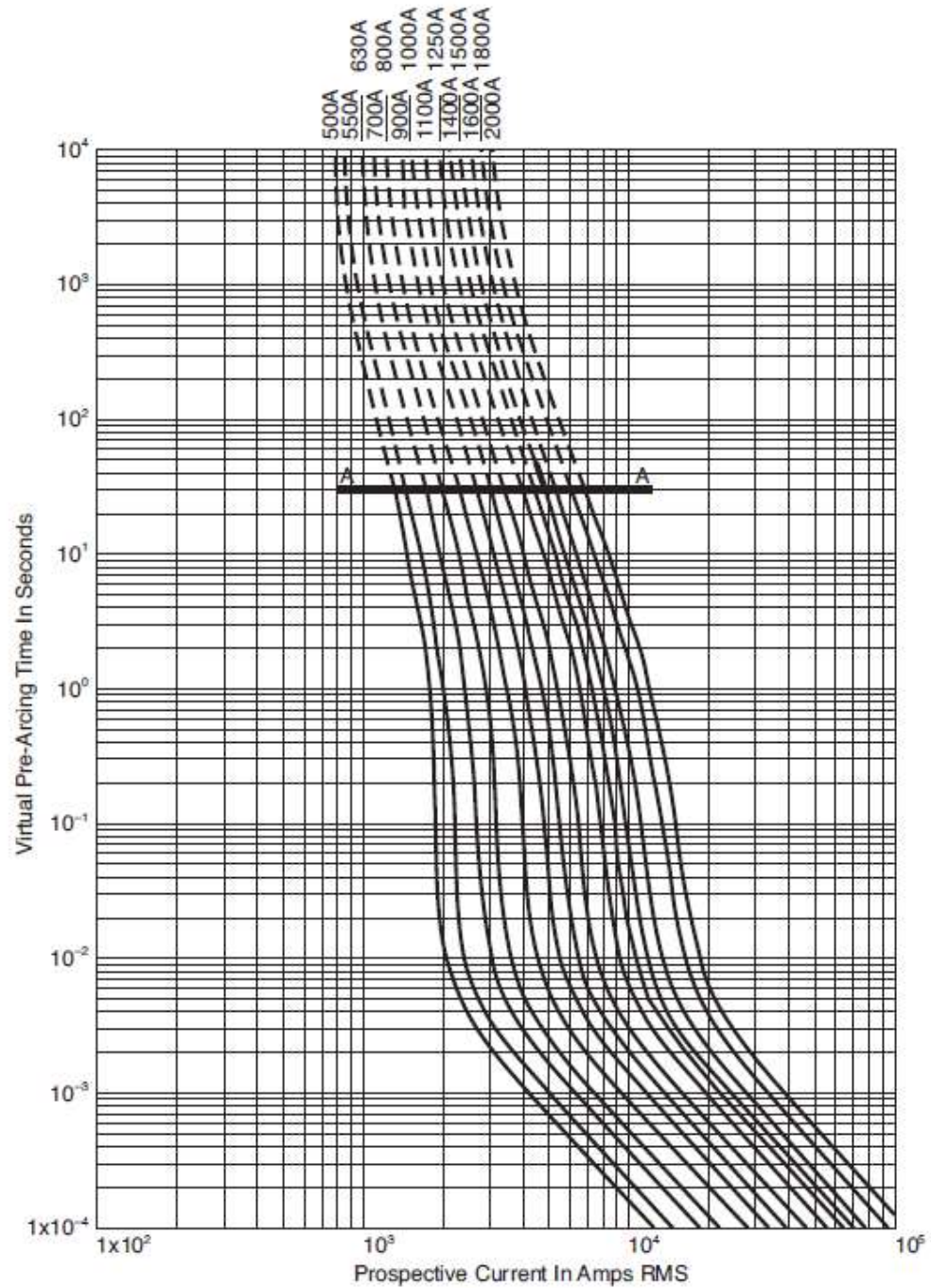*Distributed Generators.* Retrieved from

https://pdfs.semanticscholar.org/c4b5/226bad23aa38fccd3b668e41d38f346501

bb.pdf

Time Current Curves, Fuses A-E

Size 3 — 500-2000A: 690V
Time-Current Curve

The pre-arcing characteristic shows the virtual pre-arcing time as a function of the prospective short-circuit current (symm. r.m.s. value) according to IEC 60269-1.
The fuse is for short-circuit protection.
Operation at currents resulting in pre-arcing times longer than t, indicated at A on the curve, must be avoided.

$K_b = 0.6$ $N = 1.6$ Prospective Current in Ampere r.m.s.

Time Current Curves, Fuses F-L

Size 3 — 500-2000A: 690V
Time-Current Curve

Time Current Curves, Fuses M-N

Size 3 — 315-1400A: 1250V
Time-Current Curve
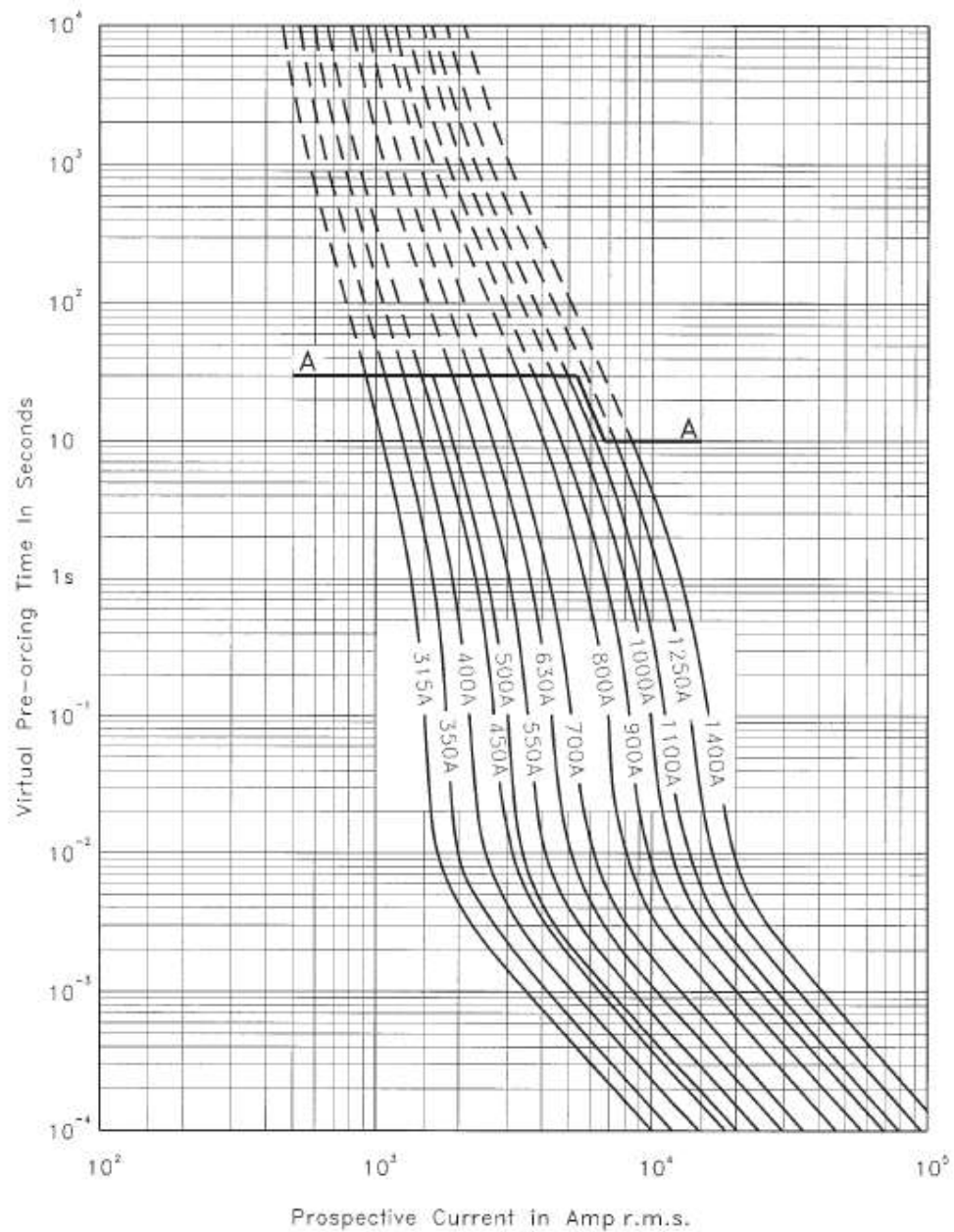
Peak Let Through Curves, Fuses A-E

Peak let-through curve
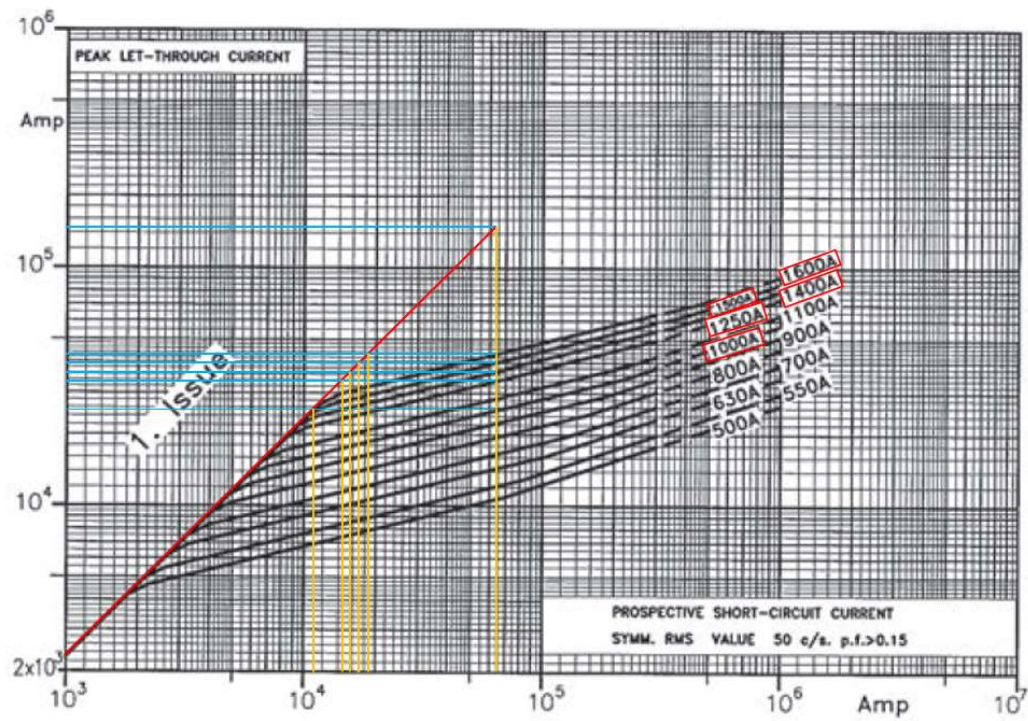
Peak Let Through Curves, Fuses F-L
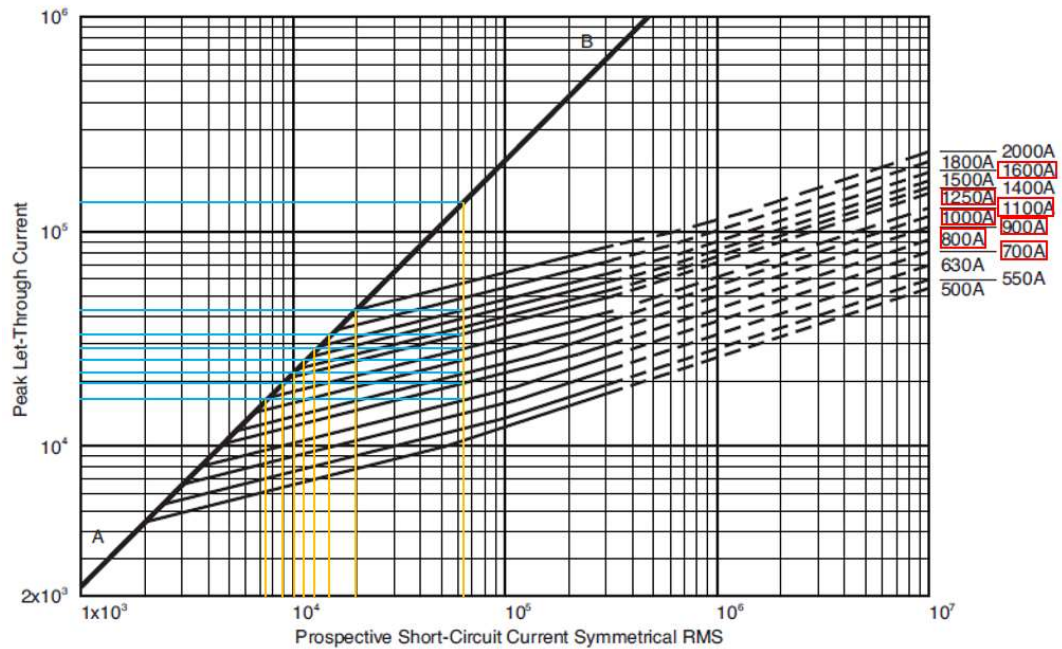
Peak Let Through Curves, Fuses M-O

Peak let-through curve
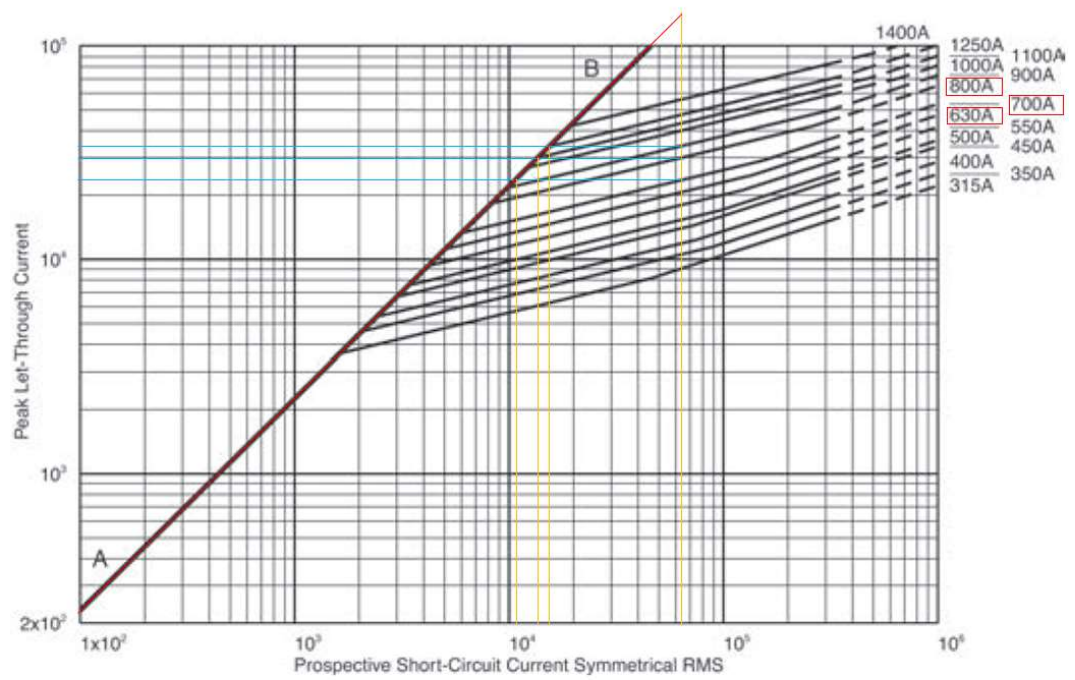
Current-carrying capacities of PVC insulated copper conductors

60364-5-52 © IEC:2009 — 49 —

Table B.52.10 – Current-carrying capacities in amperes
for installation methods E, F and G of Table B.52.1 –
PVC insulation, copper conductors –
Conductor temperature: 70 °C, reference ambient temperature: 30 °C

Nominal cross-sectional area of conductor mm²	Installation methods of Table B.52.1						
	Multi-core cables		Single-core cables				
	Two loaded conductors	Three loaded conductors	Two loaded conductors touching	Three loaded conductors trefoil	Three loaded conductors, flat		
					Touching	Spaced	
						Horizontal	Vertical
	Method E	Method E	Method F	Method F	Method F	Method G	Method G
1	2	3	4	5	6	7	8
1,5	22	18,5	–	–	–	–	–
2,5	30	25	–	–	–	–	–
4	40	34	–	–	–	–	–
6	51	43	–	–	–	–	–
10	70	60	–	–	–	–	–
16	94	80	–	–	–	–	–
25	119	101	131	110	114	146	130
35	148	126	162	137	143	181	162
50	180	153	196	167	174	219	197
70	232	196	251	216	225	281	254
95	282	238	304	264	275	341	311
120	328	276	352	308	321	396	362
150	379	319	406	356	372	456	419
185	434	364	463	409	427	521	480
240	514	430	546	485	507	615	569
300	593	497	629	561	587	709	659
400	–	–	754	656	689	852	795
500	–	–	868	749	789	982	920
630	–	–	1 005	855	905	1 138	1 070

NOTE 1 Circular conductors are assumed for sizes up to and including 16 mm². Values for larger sizes relate to shaped conductors and may safely be applied to circular conductors.

NOTE 2 D_e is the external diameter of the cable.

Current-carrying capacities of PVC insulated aluminium conductors

– 50 – 60364-5-52 © IEC:2009

Table B.52.11 – Current-carrying capacities in amperes
for installation methods E, F and G of Table B.52.1 –
PVC insulation, aluminium conductors –
Conductor temperature: 70 °C, reference ambient temperature: 30 °C

Nominal cross-sectional area of conductor mm^2	Installation methods of Table B.52.1						
	Multi-core cables		Single-core cables				
	Two loaded conductors	Three loaded conductors	Two loaded conductors touching	Three loaded conductors trefoil	Three loaded conductors, flat		
					Touching	Spaced	
						Horizontal	Vertical
	Method E	Method E	Method F	Method F	Method F	Method G	Method G
1	2	3	4	5	6	7	8
2,5	23	19,5	–	–	–	–	–
4	31	26	–	–	–	–	–
6	39	33	–	–	–	–	–
10	54	46	–	–	–	–	–
16	73	61	–	–	–	–	–
25	89	78	98	84	87	112	99
35	111	96	122	105	109	139	124
50	135	117	149	128	133	169	152
70	173	150	192	166	173	217	196
95	210	183	235	203	212	265	241
120	244	212	273	237	247	308	282
150	282	245	316	274	287	356	327
185	322	280	363	315	330	407	376
240	380	330	430	375	392	482	447
300	439	381	497	434	455	557	519
400	–	–	600	526	552	671	629
500	–	–	694	610	640	775	730
630	–	–	808	711	746	900	852

NOTE 1 Circular conductors are assumed for sizes up to and including 16 mm^2. Values for larger sizes relate to shaped conductors and may safely be applied to circular conductors.
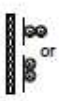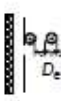
NOTE 2 D_e is the external diameter of the cable.

Metropolia
University of Applied Sciences

Current-carrying capacities of XLPE insulated copper conductors

60364-5-52 © IEC:2009 – 51 –

**Table B.52.12 – Current-carrying capacities in amperes
for installation methods E, F and G of Table B.52.1 –
XLPE or EPR insulation, copper conductors –
Conductor temperature: 90 °C, reference ambient temperature: 30 °C**

Nominal cross-sectional area of conductor mm²	Installation methods of Table B.52.1						
	Multi-core cables		Single-core cables				
	Two loaded conductors	Three loaded conductors	Two loaded conductors touching	Three loaded conductors trefoil	Three loaded conductors, flat		
					Touching	Spaced	
						Horizontal	Vertical
	Method E	Method E	Method F	Method F	Method F	Method G	Method G
1	2	3	4	5	6	7	8
1,5	26	23	–	–	–	–	–
2,5	36	32	–	–	–	–	–
4	49	42	–	–	–	–	–
6	63	54	–	–	–	–	–
10	86	75	–	–	–	–	–
16	115	100	–	–	–	–	–
25	149	127	161	135	141	182	161
35	185	158	200	169	176	226	201
50	225	192	242	207	216	275	246
70	289	246	310	268	279	353	318
95	352	298	377	328	342	430	389
120	410	346	437	383	400	500	454
150	473	399	504	444	464	577	527
185	542	456	575	510	533	661	605
240	641	538	679	607	634	781	719
300	741	621	783	703	736	902	833
400	–	–	940	823	868	1085	1008
500	–	–	1083	946	998	1253	1169
630	–	–	1 254	1 088	1 151	1 454	1 362

NOTE 1   Circular conductors are assumed for sizes up to and including 16 mm². Values for larger sizes relate to shaped conductors and may safely be applied to circular conductors.

NOTE 2 D_e is the external diameter of the cable.

Metropolia
University of Applied Sciences

Current-carrying capacities of XLPE insulated aluminium conductors

– 52 –   60364-5-52 © IEC:2009

Table B.52.13 – Current-carrying capacities in amperes
for installation methods E, F and G of Table B.52.1 –
XLPE or EPR insulation. aluminium conductors –
Conductor temperature: 90 °C, reference ambient temperature: 30 °C

Nominal cross-sectional area of conductor mm²	Installation methods of Table B.52.1						
	Multi-core cables		Single-core cables				
	Two loaded conductors	Three loaded conductors	Two loaded conductors touching	Three loaded conductors trefoil	Three loaded conductors, flat		
					Touching	Spaced	
						Horizontal	Vertical
	Method E	Method E	Method F	Method F	Method F	Method G	Method G
1	2	3	4	5	6	7	8
2,5	28	24	–	–	–	–	–
4	38	32	–	–	–	–	–
6	49	42	–	–	–	–	–
10	67	58	–	–	–	–	–
16	91	77	–	–	–	–	–
25	108	97	121	103	107	138	122
35	135	120	150	129	135	172	153
50	164	146	184	159	165	210	188
70	211	187	237	206	215	271	244
95	257	227	289	253	264	332	300
120	300	263	337	296	308	387	351
150	346	304	389	343	358	448	408
185	397	347	447	395	413	515	470
240	470	409	530	471	492	611	561
300	543	471	613	547	571	708	652
400	–	–	740	663	694	856	792
500	–	–	856	770	806	991	921
630	–	–	996	899	942	1 154	1 077

NOTE 1 Circular conductors are assumed for sizes up to and including 16 mm². Values for larger sizes relate to shaped conductors and may safely be applied to circular conductors.

NOTE 2 D_e is the external diameter of the cable.

Metropolia
University of Applied Sciences